THE UNIVERSITY OF QUEENSLAND

AUSTRALIA

KINETIC MONTE CARLO SIMULATION OF MIXTURES:

PHASE EQUILIBRIA

SHILIANG JOHNATHAN TAN

BEng (Chem)

A thesis submitted for the degree of Master of Philosophy at

The University of Queensland in 2015

School of Chemical Engineering

Abstract

This thesis deals with a development of a number of novel schemes based on kinetic Monte Carlo (*kMC*) simulation. The advantages of *kMC*, as compared to the conventional Monte Carlo are: (1) the determination of chemical potential (a fundamental thermodynamic variable) with the *kMC* scheme is more accurate than the Widom method used in the conventional (Metropolis) Monte Carlo, and (2) the *kMC* algorithm is rejection-free, making its implementation simpler. The aim of this MPhil research is to extend the *kMC* method to other ensembles including: *NPT* (isothermal-isobaric systems), μVT (constant chemical potential, volume and temperature) also known as grand canonical (GC), and to the phase-coexistence of bulk fluids (Gibbs ensemble), which are of significant interest in chemical engineering. For the first time, a new scheme using *NPT-kMC* was developed to determine accurate chemical potentials for mixtures as these are used as input in the simulation of mixtures in open systems (*GC-kMC*). Consistency between the results obtained with *NPT-kMC* and *GC-kMC* had been achieved. Finally to address the phase equilibria of bulk fluid mixtures, Gibbs ensemble *kMC* was developed as a potential alternative to the Metropolis method *Gibbs-MC*, and once again the advantage of *Gibbs-kMC* is the accurate determination of chemical potential of the two existing phases, especially for systems having a dense liquid phase where the conventional *MC* fails.

Declaration by author

This thesis is composed of my original work, and contains no material previously published or written by another person except where due reference has been made in the text. I have clearly stated the contribution by others to jointly-authored works that I have included in my thesis.

I have clearly stated the contribution of others to my thesis as a whole, including statistical assistance, survey design, data analysis, significant technical procedures, professional editorial advice, and any other original research work used or reported in my thesis. The content of my thesis is the result of work I have carried out since the commencement of my research higher degree candidature and does not include a substantial part of work that has been submitted to qualify for the award of any other degree or diploma in any university or other tertiary institution. I have clearly stated which parts of my thesis, if any, have been submitted to qualify for another award.

I acknowledge that an electronic copy of my thesis must be lodged with the University Library and, subject to the policy and procedures of The University of Queensland, the thesis be made available for research and study in accordance with the Copyright Act 1968 unless a period of embargo has been approved by the Dean of the Graduate School.

I acknowledge that copyright of all material contained in my thesis resides with the copyright holder(s) of that material. Where appropriate I have obtained copyright permission from the copyright holder to reproduce material in this thesis.

Publications during candidature

Peer-reviewed papers

1. D. D. Do, **ShiLiang (Johnathan) Tan**, Yonghong Zeng, Chunyan Fan, Van T. Nguyen, Toshihide Horikawa and D. Nicholson, *The Interplay between Molecular Layering and Clustering in Adsorption of Gases on Graphitized Thermal Carbon Black- Spill-Over Phenomenon and the Important Role of Strong Sites*. J. Colloid and Interface Science, 2015. 446: p. 98-113.

2. Van T. Nguyen, **ShiLiang (Johnathan) Tan**, D. D. Do and D. Nicholson, *Application of Kinetic Monte Carlo Method to the Vapour-Liquid Equilibria of Associating Fluids and their Mixtures,* Molecular Simulation, 2015 (In Press).

3. **ShiLiang (Johnathan) Tan**, D. D. Do and D. Nicholson, *Molecular simulation of chemical potentials of gaseous and liquid mixtures with a novel NPT-kinetic Monte Carlo simulation method,* Molecular Physics, 2015 (In press).

4. Y. Zeng, **ShiLiang (Johnathan) Tan**, D. D. Do and D. Nicholson, *Hysteresis and Scanning Curves of a Mesoporous Linear Array of Two Cavities and Three Necks*, Colloids and Surfaces A: Physicochem. Eng. Aspects, 2015 (In press).

5. **ShiLiang (Johnathan) Tan**, D. D. Do and D. Nicholson, *Development of a Grand Canonical-kinetic Monte Carlo Scheme for Simulation of Mixtures*, J. Phys. Chem., 2015 (Submitted).

6. **ShiLiang (Johnathan) Tan**, D. D. Do and D. Nicholson, *A Novel Kinetic Monte Carlo Scheme based on Gibbs ensemble to Determine Vapour-Liquid Equilibria* (In preparation).

7. **ShiLiang (Johnathan) Tan**, L. Prasetyo, Y. Zeng, P. Phadungbut, D. D. Do and D. Nicholson, *Undulation, Liquid Bridge and Adsorbate Restructuring in the Hysteresis in Open End and Closed End Pores,* Adsorption (In preparation).

Conference abstracts (speaker is underlined)

1. D. D. Do, **ShiLiang (Johnathan) Tan**, Y. Zeng, P. Phadungbut, L. Prasetyo, C. Fan, N. Klomkliang and D. Nicholson. *Mechanisms of Adsorption and Desorption of Simple Gases and Associating Fluids on Surfaces and in Confined Spaces of Porous Carbon.* Pacific Basin Conference on Adsorption Science and Technology, 24-27 September 2015, Xiamen, China

2. **ShiLiang (Johnathan) Tan**, D. D. Do and D. Nicholson, *An Efficient Method to determine Chemical Potential of Mixture with Isothermal and Isobaric (NPT) Ensemble of Kinetic Monte Carlo Simulation*, CTCMS Symposium, 21 May 2015, Queensland, Australia.

3. D. D. Do, Y. Zeng, L. Prasetyo, **ShiLiang (Johnathan) Tan**, T. Horikawa, V. Nguyen & D. Nicholson, *Characterization of Functional Group on Carbon Surface & Pattern of Isosteric Heat versus Loading*, OzCarbon, 7-12 December 2014, Adelaide, Australia

Publications included in this thesis

1. **ShiLiang (Johnathan) Tan**, D. D. Do and D. Nicholson, *Molecular simulation of chemical potentials of gaseous and liquid mixtures with a novel NPT-kinetic Monte Carlo simulation method*, Molecular Physics, 2015 (In press)

2. **ShiLiang (Johnathan) Tan**, D. D. Do and D. Nicholson, *Development of a Grand Canonical-kinetic Monte Carlo Scheme for Simulation of Mixtures*, J. Phys. Chem., 2015 (Submitted)

3. **ShiLiang (Johnathan) Tan**, D. D. Do and D. Nicholson, *A Novel Kinetic Monte Carlo Scheme based on Gibbs ensemble to Determine Vapour-Liquid Equilibria*. (In preparation)

Contribution to the authorship:

1. **ShiLiang (Johnathan) Tan**, D. D. Do and D. Nicholson, *Molecular simulation of chemical potentials of gaseous and liquid mixtures with a novel NPT-kinetic Monte Carlo simulation method*, Molecular Physics, 2015 (In press)

Contributor	Statement of contribution
Author ShiLiang Johnathan Tan (Candidate)	Simulation (100%) Wrote and edited the paper (70%)
Author Duong D. Do	Edited the paper (20%)
Author David Nicholson	Edited the paper (10%)

2. **ShiLiang (Johnathan) Tan,** D.D. Do and D. Nicholson, *Development of a Grand Canonical-kinetic Monte Carlo Scheme for Simulation of Mixtures*, J. Phys. Chem., 2015 (Submitted)

Contributor	Statement of contribution
Author ShiLiang Johnathan Tan (Candidate)	Simulation (100%) Wrote and edited the paper (70%)
Author Duong D. Do	Edited the paper (20%)
Author David Nicholson	Edited the paper (10%)

4. **ShiLiang (Johnathan) Tan**, D. D. Do and D. Nicholson, *A Novel Kinetic Monte Carlo Scheme based on Gibbs ensemble to Determine Vapour-Liquid Equilibria*. (In preparation)

Contributor	Statement of contribution
Author ShiLiang Johnathan Tan (Candidate)	Simulation (100%) Wrote and edited the paper (70%)
Author Duong D. Do	Edited the paper (20%)
Author David Nicholson	Edited the paper (10%)

Contributions by others to the thesis

None

Statement of parts of the thesis submitted to qualify for the award of another degree

None

Acknowledgements

I would like to take this oppounity to thank my principal supervisor, Professor Duong Do, without him, this thesis will not be possible. I really appreciate what he has done, going an extra miles to help me as much as he could. He has been so patient towards a person like me is commendable, for any write up I submitted is always drowned with remarks and edits in the first few version which is always depressing to look at. However, his words are always encouranging and helpful. He is the greatest mentor one could ever had.

I would also like to extend my appreciation to my co-supervisor, Professor David Nicholson for his useful comments, remarks and guidance in the completion of this thesis.

I would like to express my gratitude to the team; YongHong Zeng, Poomiwat Phadungbut and Nikom Klomkliang who help me and share their experience in simulation and experiments, and Luisa Prasetyo for keeping the spirit of the team up and fun to be in.

Thanks to my wife, Hee Xiao Xin, for supporting me throughout my studies, listening to all my blabbering. My family and my cousin, for supporting me with my undergraduate studies, as without it, this postgraduate study would not have been be possible.

Keywords

molecular simulation, kinetic monte carlo, isobaric-isothermal ensemble, NPT, grand canonical, gibbs canonical, chemical potential, mixture

Australian and New Zealand Standard Research Classifications (ANZSRC)

ANZSRC code: 090499 Chemical Engineering not elsewhere classified, 40%

ANZSRC code: 030603 Physical Chemistry Colloid and Surface Chemistry, 20%

ANZSRC code: 030799 Theoretical and Computational Chemistry not elsewhere classified, 40%

Fields of Research (FoR) Classification

FoR code: 0904 Chemical Engineering, 40%

FoR code: 0306 Physical Chemistry, 20%

FoR code: 0307 Theoretical and Computational Chemistry, 40%

Table of contents

Abstract i

Publications during candidature iii

Acknowledgements vii

Table of contents ix

List of Figures xi

List of Tables xiv

List of Abbreviations xv

Chapter 1. Introduction 1

References 2

Chapter 2. Literature review 3

2.1. Molecular simulation 4

2.1.1. Potential models 5

2.1.2. Pressure 6

2.2. Kinetic Monte Carlo Simulation 7

2.2.1. Molecular Energy 7

2.2.2. Chemical potential 7

2.3. Canonical ensemble 9

2.4. Sub-canonical ensemble 10

2.5. Special consideration 11

References 11

Chapter 3. Isothermal-Isobaric kinetic Monte Carlo 13

3.1. Introduction 13

3.2. Simulation Details 13

3.3. Setting Maximum Delta Volume 14

3.4. A new method of averaging pressure and density 15
3.5. Instant or *Block Average* Pressure? 16
3.6. Random or sequential scheme for volume move 17
3.7. Size of a *sub-NVT* block 18
3.8. Application to pure fluids and mixtures 20
3.8.1. Pure fluid: Argon at 120K and 240K 20
3.8.2. Mixtures: CH_4/ C_2H_6, CH_4/C_3H_8 and CH_4/ C_2H_6 /C_3H_8 at 300K 21
References 23
Chapter 4. Grand Canonical kinetic Monte Carlo 24
4.1. Introduction 24
4.2. Simulation Details 24
4.3. Size of a *sub-NVT* block 26
4.4. Application to pure gas and mixtures 27
References 29
Chapter 5. Gibbs Canonical kinetic Monte Carlo 30
5.1. Introduction 30
5.2. Simulation Details 31
5.3. The size of a *sub-NVT* block 33
5.4. Percentage of exchange and volume change moves 34
5.5. Scheme for volume change move 35
5.6. *Block average* activity or logarithm of block average activity 36
5.7. Application to Argon 36
References 37
Chapter 6. Conclusions and Recommendations 38
6.1. Conclusions 38
6.2. Recommendations 39

List of Figures

Figure 2-1 Illustration of periodic boundary condition, the simulation box represents solid line and its images are in dashes. 4

Figure 2-2 The working range of NVT, NPT, GC and Gibbs-NVT ensemble 5

Figure 2-3 Illustration of the new procedure with *sub-NVT* ensembles 10

Figure 3-1 The effect of constant ΔV_{max} with different magnitude. 14

Figure 3-2 (a) Volume distribution with constant ΔV_{max}; (b) Volume distribution with dynamic ΔV_{max}. 15

Figure 3-3 Plots of reduced pressure versus density of argon at 120K. (a) Pressure and density calculated from averaging the *block averages*. (b) Pressure and density calculated from time averaging over the whole simulation. Solid line with symbols: calculated pressures, symbols: specified pressure. 16

Figure 3-4 Plots of pressure versus the number of configurations. Filled circles are the block average pressure, unfilled triangles the instantaneous pressure. The solid horizontal line is the specified input pressure. 16

Figure 3-5 Ensemble average pressure against number of cycles during the sampling stage. Solid line: volume change decision made with instant pressures. Dashed line: volume change decision made with *block average* pressures. The horizontal dotted line is the specified pressure. 17

Figure 3-6 Volume against number of configurations. Unfilled circles represent the results obtained from the fix block size method and filled circles represent results obtained from the random block size method. 18

Figure 3-7 The *block average* pressure of different block size 19

Figure 3-8 Accumulative time average pressure profile of different liquid density 19

Figure 3-9 (a) Volume against the number of blocks for the final 2000 blocks; (b) Ensemble *block average* pressure using Equation 3-4 against number of configurations. The horizontal dotted line is the specified pressure. The numbers of displacement moves are: Curve 1:50k; Curve 2: -15k; Curve 3: 5k 20

Figure 3-10 Simulated properties of argon (a) Pressure at 120K; (b) Chemical potential at 120K; (c) Pressure at 240K and (d) Chemical potential at 240K as functions of density. Circles are results obtained from *NPT-kMC*, the solid line is taken from Tegeler *et al.* [1] and the dotted line is plotted from the EOS of Johnson *et al.*[2]**.** 21

Figure 3-11 (a) Pressure plot of methane/ethane mixture (dashed line) and methane/propane mixture (solid line). The symbols show the input pressure. (b) Chemical potentials of methane/ethane mixture; and (c) Chemical potentials of methane/propane mixture.....22

Figure 3-12 Chemical potential versus total density for a of methane/ethane/propane mixture. Solid line: *NPT-kMC* results; dashed line ideal gas chemical potential. The dotted line is the chemical potential of the pure component.....23

Figure 4-1 Evolution of activity with configuration 27

Figure 4-2 The *block average* activity of different block size.....27

Figure 4-3 Simulated properties for argon at (a) 240K and (b) 400K, reduced pressure (unfilled shapes) and chemical potential (filled shapes) as functions of total reduced density. Triangles are results obtained from *GC-kMC* and solid lines with circles are results obtained from *NPT*-kMC. 28

Figure 4-4 Simulated reduced pressure (unfilled shapes) and chemical potential (filled shapes) at 400K as functions of total density for (a) Methane (triangle); (b) Ethane (square); (c) Propane (diamond); and (d) methane/ethane/propane mixture. Red symbols are results from *GC-kMC* and lines with black symbols are obtained from *NPT-kMC*.....29

Figure 5-1 Van der Waals loop (a) with three distinct branches and (b) dependency on box size 30

Figure 5-2 Accumulative time average (a) activity and (b) pressure of a series of temperatures against number of configurations.....34

Figure 5-3 Series of different percentage of exchange move at 120K, the simulations uses *block average* pressure for volume move decision and activity with Rosenbluth selection for exchange move decision. 35

Figure 5-4 Different schemes for volume change move at 120K. The black vertical line represent the density of coexisting liquid and gas argon by Tegeler *et al.* [6] at 120K. 35

Figure 5-5 Different schemes for exchange move at 120K 36

Figure 5-6 Liquid-vapour equlibrium of argon, triangles and circles are the results obtained by *GEkMC* using the *block average* pressure (triangle) and ensemble average of the *block average* pressure (circle) for the decision of volume change move, crosses are results obtained by *GEMC* simulation done by Panagiotopoulos *et al.* [3] and solid line refers to Tegeler *et al.* [2]. 37

List of Tables

Table 2-1 Molecular parameters of argon model [13] and TraPPE models for methane, ethane and propane [14] 6

Table 4-1 Dimensions of the simulation box. *Density was determined from *NPT-kMC* simulations 28

List of Abbreviations

Abbreviations	**Definitions**
MC	Monte Carlo
kMC	Kinetic Monte Carlo
NVT	Constant **N**umber of particles, **V**olume and **T**emperature
NPT	Constant **N**umber of particles, **P**ressure and **T**emperature
μVT	Constant chemical potential, **V**olume and **T**emperature
GC	Grand Canonical
MD	Molecular Dynamics
EOS	Equation of state
LRC	Long range correction
aux	Auxiliary
SD	Standard deviation
Symbols	**Definitions**
R_{Cutoff}	Cut-off radius (m)
T	Temperature (K)
V	Volume (m^3)
P	Pressure (Pa)
ρ	Density (mol/m^3)
μ	Chemical potential (kJ/mol)
σ	Collision diameter (m)
ε	Well depth of interaction energy
φ	Pairwise interaction energy (kJ)
i, j, k	Counter for molecules
S	Total number of interaction sites
n, m	Counter for sites
r	Distance between sites (m)
N	Total number of molecules
u	Total molecular energy (kJ)
k_B	Boltzmann constant (kJ/mol/K)
v	Mobility of a molecule

R	Total mobility of a system
Δt	Duration of a configuration
$rand$	Random number
β	Component
Nc	Total number of component
M	Total number of configurations
Λ	Thermal de Broglie wavelength (m)
α	Activity
x, y, z	Coordinates of a molecule
Lx, Ly, Lz	Linear dimensions of a simulation box (m)
R_{matrix}	Rotation matrix
q	Eulerian angles
X	Thermodynamic property
T_M	Total time
ΔV_{max}	Maximum change in volume (m)
N_{Block}	Total number of *sub-NVT* blocks
γ	Molecular activity
Ω	Counter for boxes

Chapter 1. Introduction

Many theories have existed to describe adsorption processes on a surfaces. Irving Langmuir was the first in 1917 to describe mono-layer adsorption [1] and his theory has been extended by many scientists. One of the most popular theories in this extension is the BET theory [2], which was developed by Brunauer, Emmett and Teller in 1938. It is able to describe multilayer adsorption, an improvement from Langmuir's theory which ignores any interaction between particles (in the context of molecular simulation particle refers to a molecule, and this term will be used throughout the text). These theories encounter significant limitations, even for the description of the adsorption of simple species such as argon or nitrogen. This becomes more apparent for polyatomic molecules and for simple molecules with electrostatic interactions.

The level of increasing electrostatic interactions for the adsorbates increases as follows; argon, nitrogen, carbon dioxide, methanol, ammonia and water. The interplay between the adsorbate interaction and the solid-fluid interaction makes adsorption an interesting problem to study at the fundamental level. The phase equilibria and adsorption of simple fluids on carbon has been extensively reported in the literature but the number of studies done on associating fluids and mixtures is scarce. This is because the fundamental understanding of associating fluid alone has not been well established and its interaction with functional groups, in addition to its interaction with the graphene layers. Simulation studies showed a similar trend because associating fluids cost more computing time as the complexity of fluid increases. However, with the rapid improvement in computer hardware and software, the simulation time required has been drastically reduced, paving the way for applying computer simulation to investigate complex systems. The difficulty of making accurate determination of the chemical potential is another reason for the limited number of simulation studies on associating fluids and mixtures.

The grand canonical Monte Carlo is commonly used as a tool to simulate open systems of bulk fluid and adsorption. However, it requires the chemical potential as an input which must be obtained for a given temperature and pressure. For single atom model such as argon, the chemical potential can be calculated from an equation of state, such as that of Johnson *et al.* [1] for Lennard-Jones molecules, or those presented in Lotfi *et al*. [2]. For molecules other than single Lennard-Jones fluid, such equations of state are not readily available and to overcome such deficiency, it is common to assume that the external phase is an ideal gas.

However, this approach is unlikely to give a good estimate of chemical potential when the fluid is non-ideal, where they exhibits predominantly non-dispersion forces of interaction. Therefore, the objective of this work is to develop a novel scheme of *NPT* in the form of kinetic Monte Carlo (*kMC*) in order to accurately determine the chemical potential of complex molecules as well as mixtures. This work also extends the use of *GC-kMC* to mixtures so as to validate the chemical potential determined from *NPT-kMC*. Finally, the Gibbs ensemble *kMC* was developed as an alternative to the Gibbs-NVT to simulate phase equilibria of bulk fluid.

All simulations in this thesis is self-developed object orientated programing in Fortran 95. This thesis is constructed as follows: Chapter 2 gives an overview of kinetic Monte Carlo simulation, including the details for molecular simulation and the common algorithm for *kMC* simulation. The algorithm for *NPT-kMC* and the simulation results for bulk fluid properties will be presented in Chapter 3. The validation of the *NPT-kMC* results by using them as input for *GC-kMC* is presented in Chapter 4. Then, to complete the picture of phase studies, the *Gibbs-NVT* presented in Chapter 5 is applied to the simulation of the phase equilibria of bulk fluids. Finally, conclusions and suggestions for future work are given in Chapter 6.

References

1. Langmuir, I., *The constitution and fundamental properties of solids and liquids. II. Liquids.* Journal of the American Chemical Society, 1917. **39**(9): p. 1848-1906.
2. Brunauer, S., P. H. Emmett, and T. Edward, *Adsorption of gases in multimolecular layers.* Journal of the American Chemical Society, 1938. **60**: p. 309 - 319.
3. Johnson, J. K., J. A. Zollweg, and K. E. Gubbins, *The Lennard-Jones Equation of State Revisited.* Molecular Physics, 1993. **78**(3): p. 591-618.
4. Lotfi, A., J. Vrabec, and J. Fischer, *Vapor-Liquid-Equilibria of the Lennard-Jones Fluid from the Npt Plus Test Particle Method.* Molecular Physics, 1992. **76**(6): p. 1319-1333.

Chapter 2. Literature review

Molecular Dynamics (*MD*) and Monte Carlo (*MC*) simulations are the two most common techniques used in molecular simulations [1, 2]. *MD* is commonly applied to studies related to dynamics and *MC* is applied to equilibria. Developed by Metropolis *et al.* [3] in 1953, *MC* simulations can be run in a number of ensembles: *canonical* (constant *NVT*), isobaric-isothermal (constant *NPT*) and grand canonical (constant μVT) ensembles. Later, the Gibbs ensemble [4] (*Gibbs-NVT*) and Gibbs isobaric-isothermal [5] (*Gibbs-NPT*) was developed by Panagiotopoulos in 1987 and 1988, respectively.

In MC simulation, the importance sampling algorithm is used to decide if a trial move (e.g. displacement, rotation, volume change, insertion or deletion) is accepted or rejected. This technique however, is unsatisfactory for simulating dense systems because most trial moves are rejected. However, it can be overcome by using kinetic Monte Carlo (*kMC*) where all moves are accepted and each configuration is weighted with their time durations.

kMC was developed to study the kinetic behaviour of a system and was mostly used in simulation of crystal growth, atomic diffusion and chemical reactions. The use of *kMC* was later extended by Ustinov and Do [6], to study phase equilibria and adsorption systems [7-9], for the first time. In *kMC* simulation, the determination of chemical potential is embedded within the simulation [10], hence, no additional method or extra computing time are required to calculate the chemical potential. In Metropolis Monte Carlo, the chemical potential is calculated using the Widom method in which ghost particles are inserted in a number of frozen configurations; this is very costly because many ghost particles are required to obtain a good estimate of chemical potential. By contrast the calculated chemical potential from *kMC* is more accurate because the sampling of the configuration space is carried out with real particles.

Application of *NVT-kMC* carried out by Fan *et al.* [8] successfully describes the thermodynamic properties of nitrogen over a range of temperature and is able to describe a constant chemical potential throughout both the dilute and dense regions. This technique has later been applied to analyse associating fluids and mixtures [11]. Since *NVT-kMC* deals with closed systems, which are rare in chemical engineering, the objective of this work is to extend the *kMC* method to (1) isothermal-isobaric systems where temperature and pressure

are specified, (2) open systems where chemical potential is specified and (3) system of two coexisting phases.

2.1. Molecular simulation

Molecular simulation is an experiment done in a computer [1, 2], and one of the essential steps in a simulation is the calculation of interaction energies between molecules and also between molecules and solid bodies. To reduce simulation time, a cut-off radius, $R_{cutoff,}$ is commonly applied in the calculation of energy. To model a 3D fluid of infinite extent, we apply periodic boundary conditions in all directions as illustrated in Figure 2-1, and the minimum image convention is invoked, i.e. if the distance between the centres of mass of molecules *i* and *j* is greater than half of the length of the simulation box, the molecule *j* is replaced by its minimum image *j*'.

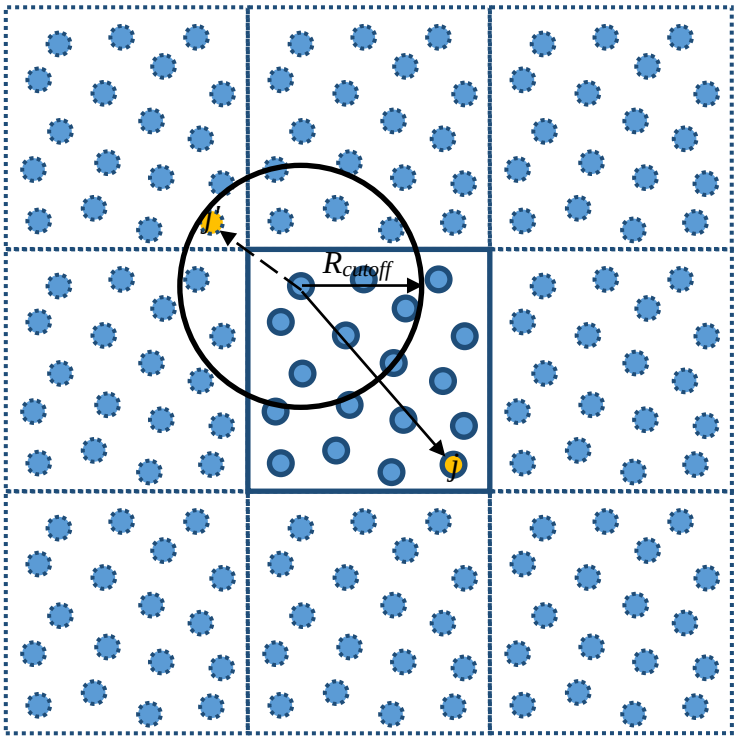

Figure 2-1 Illustration of periodic boundary condition, the simulation box represents solid line and its images are in dashes.

Different ensembles: canonical (*NVT*), Isothermal-Isobaric ensemble (*NPT*), grand canonical (GC) and Gibbs canonical ensemble (*Gibbs-NVT*) provide different output and they are summarised in Figure 2-2. The *NVT* can provide a complete van der Waals loop (vdW) of a bulk fluid at temperatures below the critical point, the *NPT* can only provide the stable and metastable states of the fluids, (either in gas or liquid phases) in terms of density versus

pressure, the *GC* is similar to *NPT*, provides the stable and metastable states in terms of density versus chemical potential and the *Gibbs-MC* provides the states of the two existing phases.

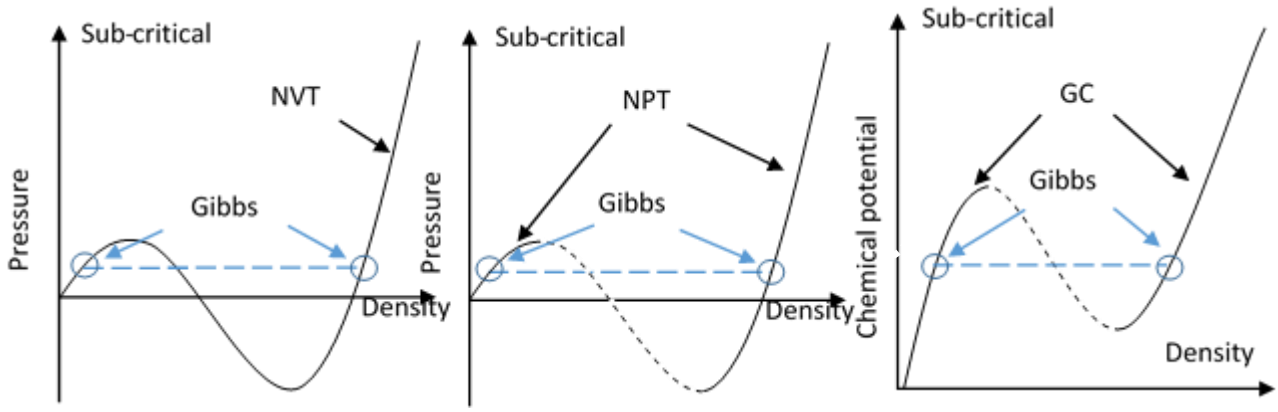

Figure 2-2 The working range of NVT, NPT, GC and Gibbs-NVT ensemble

The density, pressure, chemical potential and volume in this work are presented in reduced units by scaling them against the collision diameter or the reduced well depth as follows:

$$\begin{aligned} V_{reduced} &= V\sigma^3 \\ P_{reduced} &= \frac{P\sigma^3}{\varepsilon} \\ \rho_{reduced} &= \rho\sigma^3 \\ \mu_{reduced} &= \frac{\mu}{\varepsilon} \end{aligned} \qquad \text{Eq. 2-1}$$

2.1.1. Potential models

The molecules studied in this thesis only consist of dispersive sites described by the Lennard-Jones potential model [12]. The interaction energy between a pair of molecules *i* and *j* is calculated by:

$$\varphi_{i,j}(r) = 4\sum_{n=1}^{S_i}\sum_{m=1}^{S_j}\varepsilon^{n,m}\left[\left(\frac{\sigma^{n,m}}{r_{i,j}^{n,m}}\right)^{12} - \left(\frac{\sigma^{n,m}}{r_{i,j}^{n,m}}\right)^{6}\right] \qquad \text{Eq. 2-2}$$

where S_i and S_j is the total number of sites of molecule *i* and *j*, $r_{i,j}^{n,m}$ is the distance between site *n* on molecule *i* and site *m* on molecule *j*, $\sigma^{n,m}$ is the collision diameter and $\varepsilon^{n,m}$ is the reduced well depth calculated from the Lorentz-Berthelot mixing rule:

$$\sigma_{i,j}^{n,m} = \frac{\left(\sigma_i^n + \sigma_j^m\right)}{2}$$
$$\varepsilon_{i,j}^{n,m} = \sqrt{\varepsilon_i^n \varepsilon_j^m} \qquad \text{Eq. 2-3}$$

With the pairwise interaction energy defined, the molecular energy of a molecule *i* can be defined as:

$$u_i = \sum_{\substack{j=1 \\ j \neq i}}^{N} \varphi_{i,j} \qquad \text{Eq. 2-4}$$

Argon is used as the benchmark in this work as it is the one of the simplest molecules to simulate, and it is modelled as a sphere with a single Lennard-Jones site [13]. In reality, argon exists as an atom but in this thesis, argon is recognised as a molecule so as to be consistency with all other species modelled within this thesis. Methane, ethane and propane with molecular parameters given by Martin and Siepmann [14] are selected in this study, where methane is modelled as a single Lennard-Jones fluid while ethane and propane are modelled as multi-centered Lennard-Jones fluids. In addition, mixtures of these alkanes are studied because they are relevant in the description of natural gas properties.

	Units	**Argon**	**Methane**	**CH_2**	**CH_3**
Collision diameter (σ)	nm	0.3405	0.373	0.375	0.395
Well depth (ε)	K	119.8	148	46	98
Bond Length	nm	-	-	0.154	0.154
Bond angle	o	-	-	114	114

Table 2-1 Molecular parameters of argon model [13] and TraPPE models for methane, ethane and propane [14]

2.1.2. Pressure

The total pressure of a bulk fluid is calculated in three parts;

$$P_{Total} = P_{Ideal} + P_{Excess} + P_{LRC} \qquad \text{Eq. 2-5}$$

where the ideal gas pressure is:

$$P_{Ideal} = \rho kT \qquad \text{Eq. 2-6}$$

The excess pressure, accounts for the interaction between molecules is calculated via the virial route

$$P_{Excess} = \frac{1}{3V}\sum_{i=1}^{N-1}\sum_{j=i+1}^{N}\sum_{n=1}^{S_i}\sum_{m=1}^{S_j}\frac{\mathbf{r}_{i,j}.\mathbf{r}_{i,j}^{n,m}}{r_{i,j}^{n,m}}\frac{d\varphi(r_{i,j}^{n,m})}{dr_{i,j}^{n,m}} \qquad \text{Eq. 2-7}$$

Here, $r_{i,j}$ is the distance between the centres of molecules i and j, and $r_{i,j}^{n,m}$ is the distance between the site n of molecule i and the site m on molecule j. The final term is the long range correction for pressure because of the cut-off in the pairwise calculation of energy for molecules whose distance is greater than R_{Cutoff}.

$$P_{LRC} = \frac{16}{3}\pi\rho^2\sum_{n=1}^{S_i}\sum_{m=1}^{S_j}\varepsilon_{i,j}^{n,m}\left(\sigma_{i,j}^{n,m}\right)^3\left[\frac{2}{3}\left(\frac{\sigma_{i,j}^{n,m}}{R_{Cutoff}}\right)^9-\left(\frac{\sigma_{i,j}^{n,m}}{R_{Cutoff}}\right)^3\right] \qquad \text{Eq. 2-8}$$

2.2. Kinetic Monte Carlo Simulation

2.2.1. Molecular Energy

Given the molecular energy, u_i, of the molecule i in Equation 2-4, its mobility is defined as:

$$\nu_i = \exp\left(\frac{u_i}{k_B T}\right) \qquad \text{Eq. 2-9}$$

The total mobility of the system the sum of all the molecular mobilities:

$$R = \sum_{i=1}^{N}\nu_i = \sum_{i=1}^{N}\exp\left(\frac{u_i}{k_B T}\right) \qquad \text{Eq. 2-10}$$

Since this is a measure of how fast the system evolves, it means that the current configuration will exist, on average, for a time of:

$$\overline{\Delta t} = \frac{1}{R} \qquad \text{Eq. 2-11}$$

There are many microscopic configurations that give the same total mobility R, and therefore the duration for a configuration will follow a Poisson distribution law, i.e.

$$\Delta t = \overline{\Delta t}\ln\left(\frac{1}{rand}\right) = \frac{1}{R}\ln\left(\frac{1}{rand}\right) \qquad \text{Eq. 2-12}$$

where *rand* is a random number ($0 < rand < 1$).

2.2.2. Chemical potential

For a simulation box with a mixture of N molecules,

$$N = \sum_{\beta=1}^{N_C} N_\beta \qquad \text{Eq. 2-13}$$

where N_β is the number of molecules belonging to the component β, and N_C is the number of components.

In a *canonical kMC* simulation, the excess (configurational) chemical potential [10] of a component β is calculated as follows:

$$\mu_\beta^{ex} = kT \ln\left(\frac{\langle R_\beta \rangle}{N_\beta}\right) \qquad \text{Eq. 2-14}$$

where R_β is the total mobility rate of the component β, calculated using Equation 2-10 with only molecules of this component counted in the summation, and its time average is given by

$$\langle R_\beta \rangle = \frac{\sum_{j=1}^{M} \left(\Delta t_j \; R_{\beta,j}\right)}{\sum_{j=1}^{M} \Delta t_j} \qquad \text{Eq. 2-15}$$

Here the subscript j denotes the *j-th* configuration in a sequence of M configurations, and Δt_j is its duration, calculated with Equation 2-12, which requires the total mobility of all molecules. The chemical potential of the component β is the sum of the excess chemical potential and the ideal gas chemical potential, which is given below [15]:

$$\mu_\beta^{IG} = kT \ln\left(\frac{\Lambda_\beta^3 N_\beta}{V}\right) + \mu_\beta^{ROT} + \mu_\beta^{VIB} + \mu_\beta^{ELEC} \qquad \text{Eq. 2-16}$$

where Λ_β is the thermal de Broglie wavelength of the component β. The first term of the above equation is the chemical potential due to translation, which is a function of density, and the second, third and fourth terms are intramolecular chemical potentials due to rotation, vibration and electronic transitions, respectively. They can be lumped together as μ_β^{intra} and the chemical potential written as the sum of the ideal gas and excess chemical potentials:

$$\mu_\beta = \left[kT \ln\left(\frac{\Lambda_\beta^3 N_\beta}{V}\right) + \mu_\beta^{\text{intra}} \right] + kT \ln\left(\frac{\langle R_\beta \rangle}{N_\beta}\right) \qquad \text{Eq. 2-17}$$

which is simplified as:

$$\mu_\beta - \mu_\beta^{\text{intra}} = kT \ln\left(\frac{\Lambda_\beta^3 \langle R_\beta \rangle}{V}\right)$$
$$\mu_\beta - \mu_\beta^{\text{intra}} = kT \ln\left(\Lambda_\beta^3 \langle \alpha_\beta \rangle\right) \qquad \text{Eq. 2-18}$$

where α_β is the activity of the component β:

$$\alpha_\beta = \frac{R_\beta}{V} \qquad \text{Eq. 2-19}$$

For a given temperature and pressure, an *NPT-kMC* simulation can be carried out to determine the chemical potential and the output of this simulation is a set of $\mu_\beta - \mu_\beta^{\text{intra}}$ for all components, which is then used as input to a *GC-kMC* simulation.

2.3. Canonical ensemble

In an NVT ensemble, a chain of configurations is generated by selecting a molecule and allowing it to sample the volume space uniformly. To this end, we apply the Rosenbluth scheme [1] for selecting one molecule with high mobility but not necessarily the one with the highest mobility. First, we calculate the partial sum of the mobilities from molecule 1 to molecule *k* (inclusive), irrespective of their identity:

$$R_k = \sum_{j=1}^{k} \nu_j \qquad \text{Eq. 2-20}$$

that is, $R = R_N$. A molecule is selected (the k-*th* molecule) according to:

$$R_{k-1} \leq rand \times R < R_k \qquad \text{Eq. 2-21}$$

Once the molecule *k* is selected, it is moved to a random position within the simulation box:

$$x^{new} = Rand \times Lx$$
$$y^{new} = Rand \times Ly \qquad \text{Eq. 2-22}$$
$$z^{new} = Rand \times Lz$$

where *x*, *y* and *z* are the coordinates for the centre of the *k-th* molecule in the new position, *Lx*, *Ly* and *Lz* are the linear dimensions of the simulation box. For polyatomic molecules, the *k-th* molecule is given a new orientation using the quaternion [1] as follows:

$$R_{matrix} = \begin{bmatrix} q_0^2 + q_1^2 - q_2^2 - q_3^2 & 2\left(q_1 \bullet q_2 - q_0 \bullet q_3\right) & 2\left(q_1 \bullet q_3 + q_0 \bullet q_2\right) \\ 2\left(q_1 \bullet q_2 + q_0 \bullet q_3\right) & q_0^2 - q_1^2 + q_2^2 - q_3^2 & 2\left(q_2 \bullet q_3 - q_0 \bullet q_1\right) \\ 2\left(q_1 \bullet q_3 - q_0 \bullet q_2\right) & 2\left(q_2 \bullet q_3 + q_0 \bullet q_1\right) & q_0^2 - q_1^2 - q_2^2 + q_3^2 \end{bmatrix} \quad \text{Eq. 2-23}$$

where R_{matrix} is the rotation matrix, (q_0, q_1, q_2, q_3) is the vector on a four-dimensional unit sphere, $1 = q_0^2 + q_1^2 + q_2^2 + q_3^2$ related to the Eulerian angles by:

$$\begin{aligned} q_0 &= \cos\frac{\theta}{2}\cos\left(\frac{\phi+\psi}{2}\right) \\ q_1 &= \sin\frac{\theta}{2}\cos\left(\frac{\phi-\psi}{2}\right) \\ q_2 &= \sin\frac{\theta}{2}\sin\left(\frac{\phi-\psi}{2}\right) \\ q_3 &= \cos\frac{\theta}{2}\sin\left(\frac{\phi+\psi}{2}\right) \end{aligned} \quad \text{Eq. 2-24}$$

After the move has been executed, the molecular energies of all molecules are updated as follows:

$$u_i^{new} = \sum_{\substack{j=1 \\ j \neq k}}^{N} \varphi_{i,j}^{new} \quad \text{Eq. 2-25}$$

$$u_j^{new} = u_j^{old} + \left(\varphi_{j,i}^{new} - \varphi_{j,i}^{old}\right); \text{ for } i \neq j \quad \text{Eq. 2-26}$$

2.4. Sub-canonical ensemble

The sub-canonical ensemble is a novel procedure for carrying out the isothermal-isobaric, grand canonical and Gibbs canonical kinetic Monte Carlo simulation. It is essentially a sequence of *M* local displacements in a *sub-NVT* block, followed by a specific move of either an exchange move (as in the case of *GC-kMC* and *Gibbs-kMC*) or volume move (in *NPT-kMC* and *Gibbs-kMC*) as illustrated in Figure 2-3.

Figure 2-3 Illustration of the new procedure with *sub-NVT* ensembles

The choice of M is made in such a way that we can make a reasonable estimate of a thermodynamic property X such as pressure, density, chemical potential and energy. The time average thermodynamic properties of this *sub-NVT* block can be calculated from:

$$\langle X \rangle = \frac{\sum_{j=1}^{M} \Delta t_j \; X_j}{\sum_{j=1}^{M} \Delta t_j} = \frac{\sum_{j=1}^{M} \Delta t_j \; X_j}{T_M} = \sum_{j=1}^{M} \tau_j \; X_j \qquad \text{Eq. 2-27}$$

Hereafter, the time average of this *sub-NVT* block is called the *block average*.

2.5. Special consideration

Common to all ensembles, a molecule i might overlap significantly with other molecules. In such cases, the pairwise potential energy between this molecule and its overlapping neighbours can be a large positive number, and this can cause a floating overflow. To avoid this situation, we implement the following algorithm: If one of the site-site distances between two overlapping molecules is smaller than 0.8σ, we give the molecular pairwise potential energy a large positive value

$$\frac{\varphi_{i,j}}{\varepsilon_{i,j}} = 40 \qquad \text{Eq. 2-28}$$

for all overlapping neighbouring molecules j.

References

1. Frenkel, D. and B. Smit, *Understanding molecular simulation : From algorithms to applications.* Second ed. Computational Science Series, ed. D. Frenkel, et al. 2002, San Diego: Academic Press. 638.
2. Allen, M.P. and D.J. Tildesley *Computer Simulation of Liquids*. 1989, Oxford: Oxford University Press. xiii, 385.
3. Metropolis, N., A.W. Rosenbluth, M.N. Rosenbluth, and A.H. Teller, *Equation of state calculations by fast computing machines.* The Journal of Chemical Physics, 1953. **21**(6): p. 1087-1092.
4. Panagiotopoulos, A.Z., *Direct determination of phase coexistence properties of fluids by Monte Carlo simulation in a new ensemble.* Molecular Physics, 1987. **61**(4): p. 813-826.
5. Panagiotopoulos, A.Z., N. Quirke, M. Stapleton, and D.J. Tildesley, *Phase equilibria by simulation in the Gibbs ensemble: Alternative derivation, generalisation and application to mixture and membrane equilibria.* Molecular Physics, 1988. **63**(4): p. 527-545.
6. Ustinov, E.A. and D.D. Do, *Application of kinetic Monte Carlo method to equilibrium systems: vapour-liquid equilibria.* J Colloid Interface Sci, 2012. **366**(1): p. 216-23.

7. Ustinov, E.A. and D.D. Do, *Two-dimensional order-disorder transition of argon monolayer adsorbed on graphitized carbon black: kinetic Monte Carlo method.* J Chem Phys, 2012. **136**(13): p. 134702.
8. Fan, C., D.D. Do, D. Nicholson, and E. Ustinov, *A novel application of kinetic Monte Carlo method in the description of N2 vapour–liquid equilibria and adsorption.* Chemical Engineering Science, 2013. **90**(0): p. 161-169.
9. Ustinov, E.A. and D.D. Do, *Simulation of gas adsorption on a surface and in slit pores with grand canonical and canonical kinetic Monte Carlo methods.* Phys Chem Chem Phys, 2012. **14**(31): p. 11112-8.
10. Fan, C., D.D. Do, D. Nicholson, and E. Ustinov, *Chemical potential, Helmholtz free energy and entropy of argon with kinetic Monte Carlo simulation.* Molecular Physics, 2013. **112**(1): p. 60-73.
11. Van T. Nguyen, S.Johnathan.T., D. D. Do and D. Nicholson, *Application of Kinetic Monte Carlo Method to the Vapour-Liquid Equilibria of Associating Fluids and their Mixtures.* Molecular Simulation, 2015, DOI:10.1080/08927022.2015.1067809.
12. Jones, J.E., *On the Determination of Molecular Fields. II. From the Equation of State of a Gas.* Proceedings of the Royal Society of London. Series A, Containing Papers of a Mathematical and Physical Character, 1924. **106**(738): p. 463-477.
13. Michels, A., H. Wijker, and H. Wijker, *Isotherms of argon between 0°c and 150°c and pressures up to 2900 atmospheres.* Physica, 1949. **15**(7): p. 627-633.
14. Martin, M.G. and J.I. Siepmann, *Transferable potentials for phase equilibria. 1. United-atom description of n-alkanes.* J Phys Chem B, 1998. **102**(14): p. 2569-2577.
15. Hill, T.L., *An Introduction to Statistical Thermodynamics*. Addison-wesley serious in chemistry, ed. F.T. Bonner and G.C. Pimentel. 1960, Massachusetts, USA: Addison-wesley publishing company, inc. 508.

Chapter 3. Isothermal-Isobaric kinetic Monte Carlo

3.1. Introduction

In industry, it is common for engineers to describe the state of a system for a given pressure and temperature as they are readily measureable. To this end, a simulation of constant **N**umber of molecules, **P**ressure and **T**emperature (*NPT*) is required. During the course of a simulation in this so called *NPT* ensemble, the size of the box is changed so that the pressure calculated with the virial route matches (within a statistically error) the specified pressure. This type of simulation can determine properties in the stable and metastable regions but not the unstable region as explained earlier in Figure 2-2. In this chapter, a methodology is developed to achieve a satisfactory volume change move.

3.2. Simulation Details

There are two ways to carry out a volume change move by using either (1) the instant pressure or (2) the time average pressure of a *sub-NVT* block also known as the *block average* as in Equation 2-27. The volume move can be done in a stochastic manner or deterministically. For the former, we define an auxiliary pressure as:

$$P^{aux} = P + P^{*} \qquad \text{Eq. 3-1}$$

where P^{*} is the specified pressure. If P, the pressure, is greater than $Rand \times P^{aux}$, then the pressure is taken to be too high and the volume is increased according

$$V' = V + rand \times \Delta V_{\max} \qquad \text{Eq. 3-2}$$

where ΔV_{max} is the maximum allowable volume change. On the other hand, if P is less than $Rand \times P^{aux}$, then the instant pressure is taken to be too low and the volume is decreased

$$V' = V - rand \times \Delta V_{\max} \qquad \text{Eq. 3-3}$$

The volume change move done deterministically is as follows: if the pressure is greater than P^{*}, the volume is expanded according to Equation 3-2 and on the other hand, if it is less than P^{*}, the volume is decreased using Equation 3-3. After the volume of a box is changed, the cut-off radius is scaled accordingly to half of the new box length.

The standard protocol for performing an *NPT* simulation is as follows, unless otherwise stated: A run at 120K comprised 20000 *sub-NVT* blocks with 15000 displacement moves per block and a volume change move at the end of each block. The *block average* pressure was used to decide on the volume change. The initial volume and the number of particles were set at $27nm^3$ (cubic box) and 300, respectively.

3.3. Setting Maximum Delta Volume

In an *NPT* simulation, the maximum change in volume (ΔV_{max}) needs to be chosen with care. If it is too large there will be a large number of overlapping particles when a volume contraction is made and consequently a large number of local displacement moves would be needed to relax the system. On the other hand, if ΔV_{max} is too small, many volume change moves would be required as illustrated in Figure 3-1. Furthermore, it is found that if ΔV_{max} was kept constant throughout the whole course of simulation, it was difficult to achieve equilibrium within a reasonable simulation time.

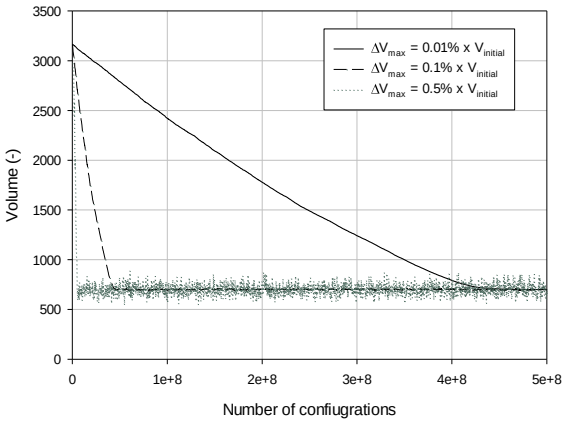

Figure 3-1 The effect of constant ΔV_{max} with different magnitude.

To overcome this problem, a dynamic change in ΔV_{max} was adopted. Initially ΔV_{max} was given a sufficiently large value that the volume of the box quickly reaches a range close to the expected value. ΔV_{max} was then reduced to a smaller value such that the calculated pressure oscillates with smaller amplitude about the specified pressure and eventually converges to this value. To find a new value for ΔV_{max} a histogram of volume was obtained, generated by summing the total *kMC* time for a given volume (*sub-NVT* block) as shown in Figure 3-2a. This volume distribution has an almost symmetrical distribution with a standard deviation (SD) that is a measure of how much the volume of the system fluctuates. This SD

was then used as a basis for the next estimate of ΔV_{max}. By trial and error, it has been found that half the standard deviation was the optimum choice. By applying this updated ΔV_{max} on the fly the simulation is able to reach the desired volume more efficiently (Figure 3-2b) than keeping it constant as illustrated in Figure 3-1. It was also noted that the value of ΔV_{max} became smaller with progress of the simulation, rendering the fluctuation in pressure smaller. This procedure gives a much more reliable estimate of the calculated pressure, density and chemical potential.

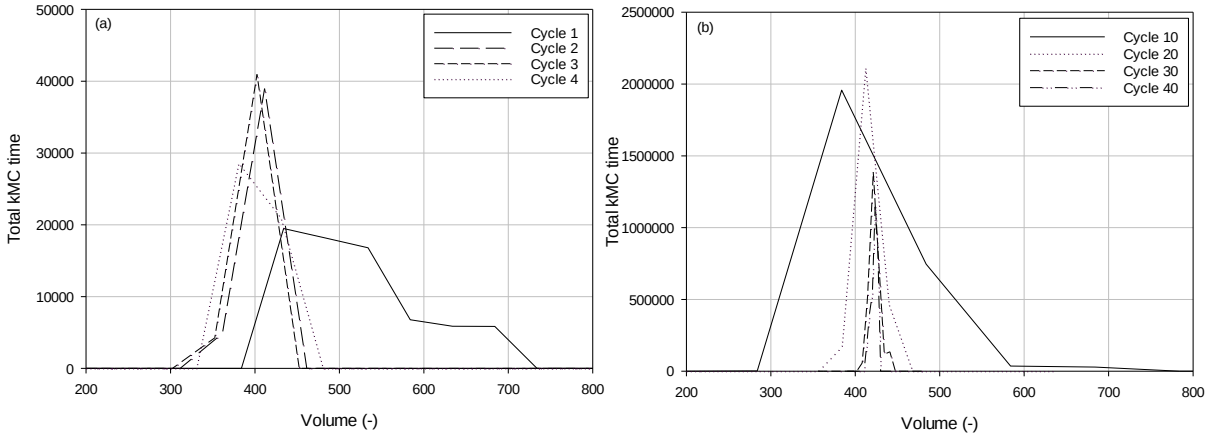

Figure 3-2 (a) Volume distribution with constant ΔV_{max}; (b) Volume distribution with dynamic ΔV_{max}.

3.4. A new method of averaging pressure and density

It was found that the calculated time-weighted average pressure given by Equation 2-27 was consistently lower than the specified pressure and therefore there is a need for a new procedure to determine the *block average* pressure and density. After one volume change has been made, the simulation is carried out in a *sub-NVT* ensemble (with only local displacements) to relax the system, from which the *block average* pressure and density can be obtained. The average pressure and density for the whole simulation was then calculated as the ensemble average of the *block average* pressures or densities:

$$\left[\langle P\rangle\right] = \frac{\sum_{n=1}^{N_{Block}} \langle P\rangle_n}{N_{Block}} \qquad \left[\langle \rho\rangle\right] = \frac{\sum_{n=1}^{N_{Block}} \langle \rho\rangle_n}{N_{Block}} \qquad \text{Eq. 3-4}$$

where N_{Block} is the number of block. Figure 3-3a shows the average pressures obtained by this procedure or by time averaging using all the instantaneous pressure (Figure 3-3b) as a

function of density. It is clear that the *block average* scheme gives much better description of the system.

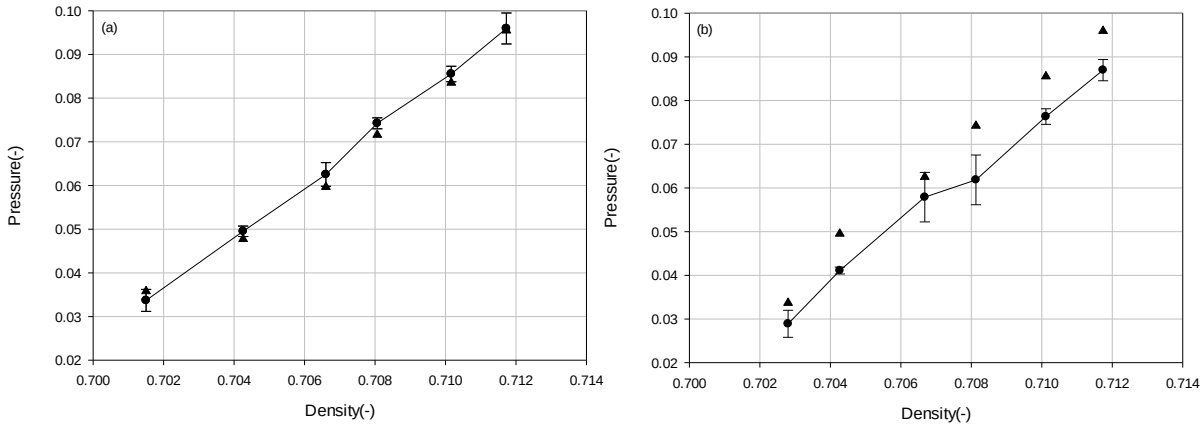

Figure 3-3 Plots of reduced pressure versus density of argon at 120K. (a) Pressure and density calculated from averaging the *block averages*. (b) Pressure and density calculated from time averaging over the whole simulation. Solid line with symbols: calculated pressures, symbols: specified pressure.

3.5. Instant or *Block Average* Pressure?

Figure 3-4 shows the instant pressure and the *block average* pressure as function of the number of configurations at 120K where the *block average* pressure was used as the decision for the volume change move. In this simulation, a *sub-NVT* block contain 100,000 local displacements instead of the standard protocol as the purpose of this simulation is to show the evolution of pressure with the number of configurations. The figure illustrates the strong fluctuations of the instant pressure about the *block average* pressure, confirming that the use of the *block average* pressure to decide the volume change move is a better choice.

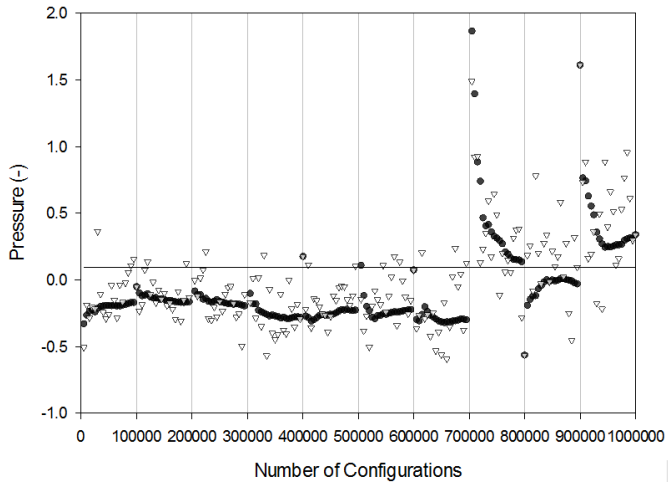

Figure 3-4 Plots of pressure versus the number of configurations. Filled circles are the block average pressure, unfilled triangles the instantaneous pressure. The solid horizontal line is the specified input pressure.

To further justify the choice of the *block average* pressure, Figure 3-5 shows that the *block average* scheme reaches equilibrium faster than the scheme using the instant pressure. Hence, the *block average* procedure was used in all subsequent simulations.

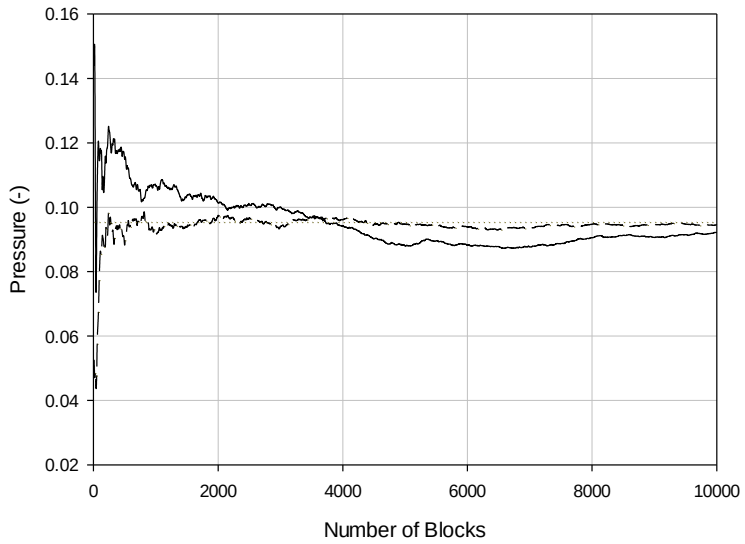

Figure 3-5 Ensemble average pressure against number of cycles during the sampling stage. Solid line: volume change decision made with instant pressures. Dashed line: volume change decision made with *block average* pressures. The horizontal dotted line is the specified pressure.

3.6. Random or sequential scheme for volume move

For a given number of local moves and volume moves, the choice of local move or volume change move can be made sequentially or in a random manner. By sequential, it is meant that a number of local moves are made in one block, followed by a volume move. This method ensures that the system has been relaxed sufficiently before a volume change move is made. The second choice retains the stochastic nature of Monte Carlo simulation by doing the volume change move at random within a set number of local displacement moves. However, there are rare occurrences where the interval between two volume change moves is very small resulting in an undesirable perturbation. Figure 3-6 shows a plot of the evolution of volume versus the number of configurations, and it is seen that there is no difference in the performance of these two methods.

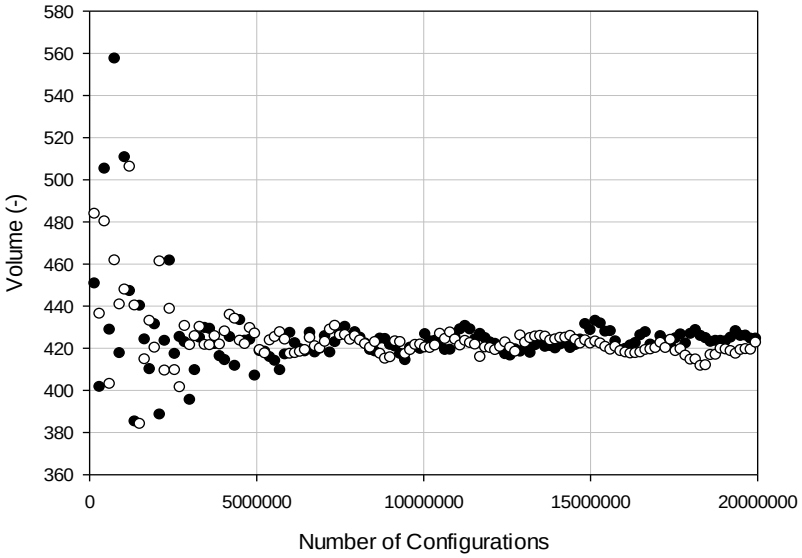

Figure 3-6 Volume against number of configurations. Unfilled circles represent the results obtained from the fix block size method and filled circles represent results obtained from the random block size method.

3.7. Size of a *sub-NVT* block

It is important that the number of displacement moves in (or the size of) a *sub-NVT* block is large enough to obtain an accurate estimation of the *block average* pressure. If the size of a *sub-NVT* block is too small, the pressure may deviate too far from the specified value and consequently the volume change is incorrectly carried out. On the other hand, an unnecessarily large *sub-NVT* block number would significantly increase the computational time taken to complete the simulation. To illustrate this point, Figure 3-7 shows the fluctuation of the *block average* pressure against the number of configurations for different choices of block size. As expected, the fluctuation is lower for larger block size but, of course, at the expense of longer computation time.

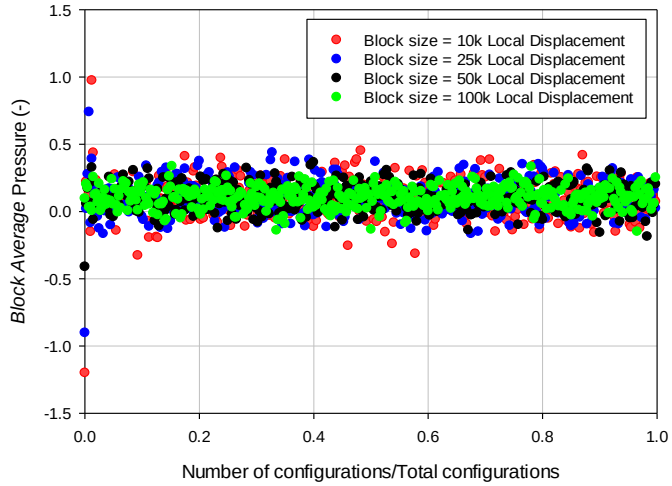

Figure 3-7 The *block average* pressure of different block size

The optimum choice of the block size depends on the density of the system. To test this to the extreme, the result for a very dense liquid argon at 120K is illustrated in Figure 3-8. The plot of the time average pressure shows that to achieve a good estimate of pressure in a single block, the block size increases with the density.

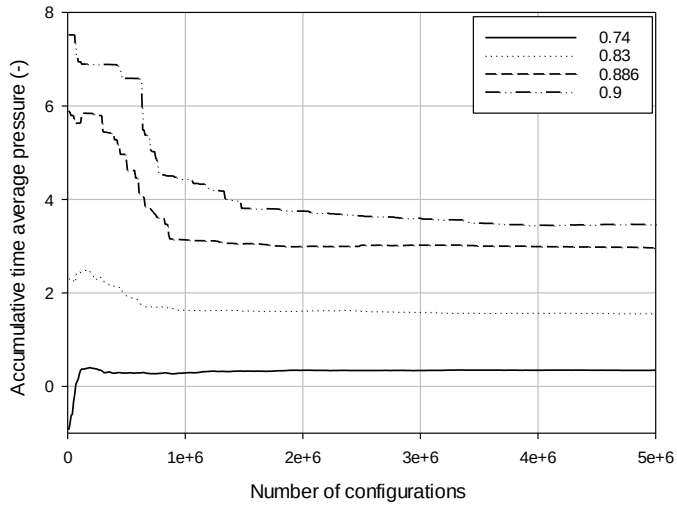

Figure 3-8 Accumulative time average pressure profile of different liquid density

In order to determine the optimum number of displacement moves, three *sub-NVT* block sizes were examined. Figure 3-9a the plot of the volume versus the number of blocks for a number of local displacement moves per block and it shows that when the number of local displacement moves is 5k, the volume profile becomes noisy. When this number is increased to 15k or to 50k, there is no significant improvement in the volume profile, suggesting that the *block average* pressures for 50k and 15k would be similar. Despite the strong volume

fluctuations for 5k local displacement moves per block, the simulation still reaches equilibrium but with lower accuracy, as seen in Figure 3-9b where the *block average* pressure is plotted against the number of configurations. The run with 50k local displacement has the smallest error, but takes the longest total CPU time. Therefore, 15k was selected as a compromise number for the number of local displacement moves per block.

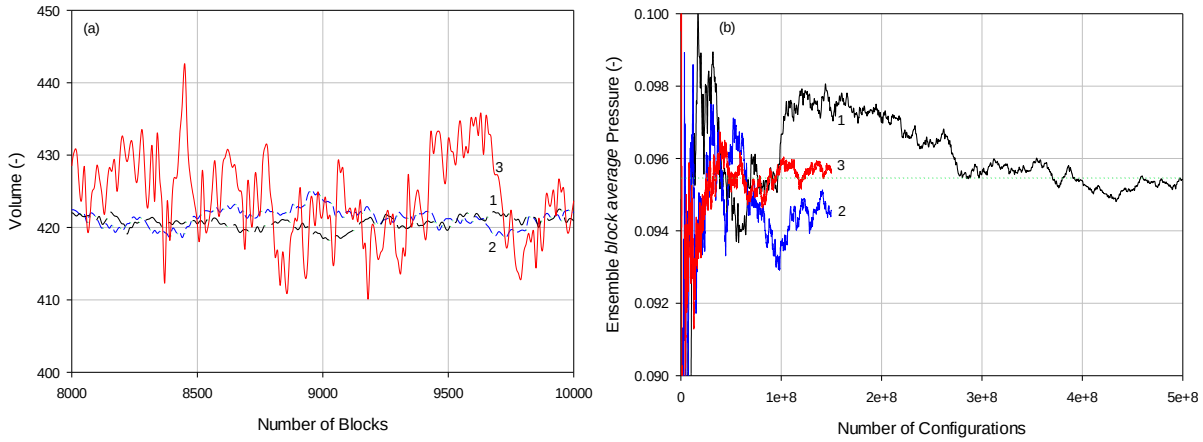

Figure 3-9 (a) Volume against the number of blocks for the final 2000 blocks; (b) Ensemble *block average* pressure using Equation 3-4 against number of configurations. The horizontal dotted line is the specified pressure. The numbers of displacement moves are: Curve 1:50k; Curve 2: -15k; Curve 3: 5k

3.8. Application to pure fluids and mixtures

3.8.1. Pure fluid: Argon at 120K and 240K

Liquid and gas phase simulations were run in a cubic box with initial linear dimensions of 3nm and 5nm, respectively, at 120K (sub-critical temperature) and at 240K (supercritical temperature) in a cubic box with the initial linear dimension of 5nm, and 300 particles. Note that the pressure and density are calculated using the ensemble average of the *block average* and the chemical potential is calculated using the time average over the whole course of simulation.

Figure 3-10 shows that the simulated density and chemical potential from *kMC-NPT* simulations are in good agreement with Tegeler *et al.* [1] and with the *EOS* of Johnson *et al.* [2] at both sub-critical (120K) and supercritical (240K) temperatures.

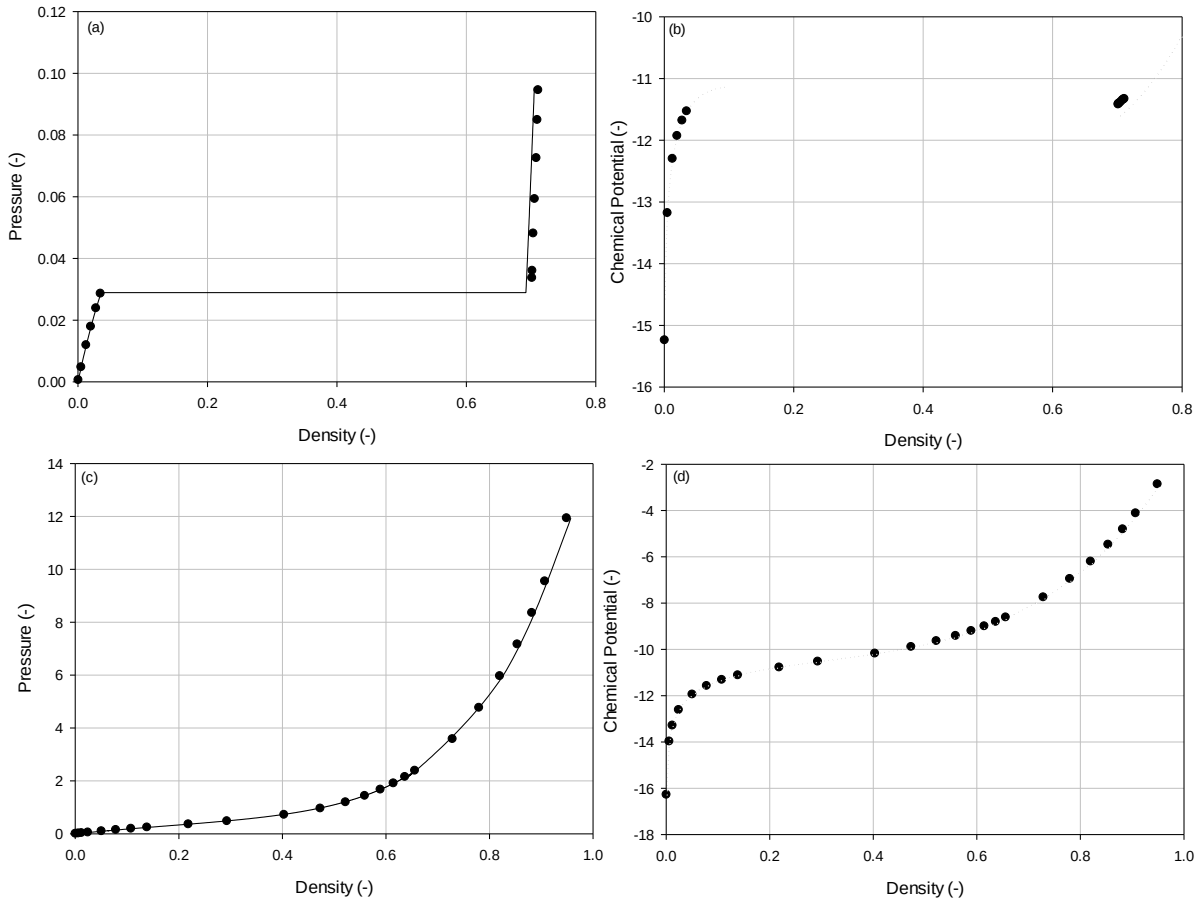

Figure 3-10 Simulated properties of argon (a) Pressure at 120K; (b) Chemical potential at 120K; (c) Pressure at 240K and (d) Chemical potential at 240K as functions of density. Circles are results obtained from *NPT-kMC*, the solid line is taken from Tegeler *et al.* [1] and the dotted line is plotted from the EOS of Johnson *et al.*[2]**.**

3.8.2. Mixtures: CH_4/ C_2H_6, CH_4/C_3H_8 and CH_4/ C_2H_6 /C_3H_8 at 300K

As examples to illustrate the potential of the *kMC-NPT* method, mixture simulations of methane, ethane and propane at 300K were carried out in a cubic box with a side length of 5nm. For the binary systems, 150 molecules were used for each species (equal mole fractions) and for the ternary systems 100 molecules for each species.

Figure 3-11a show the results in the bulk phase, and it is observed that the methane/ethane mixture has higher pressure than the methane/propane mixture because of the stronger molecular interactions in propane/methane mixture, compared to the other system. It is also seen that the calculated pressure agrees very well with the specified pressure, indicating the validity of the *NPT* scheme proposed in this thesis. Figure 3-11b and c show the chemical potentials of the methane/ethane and methane/propane mixture, respectively.

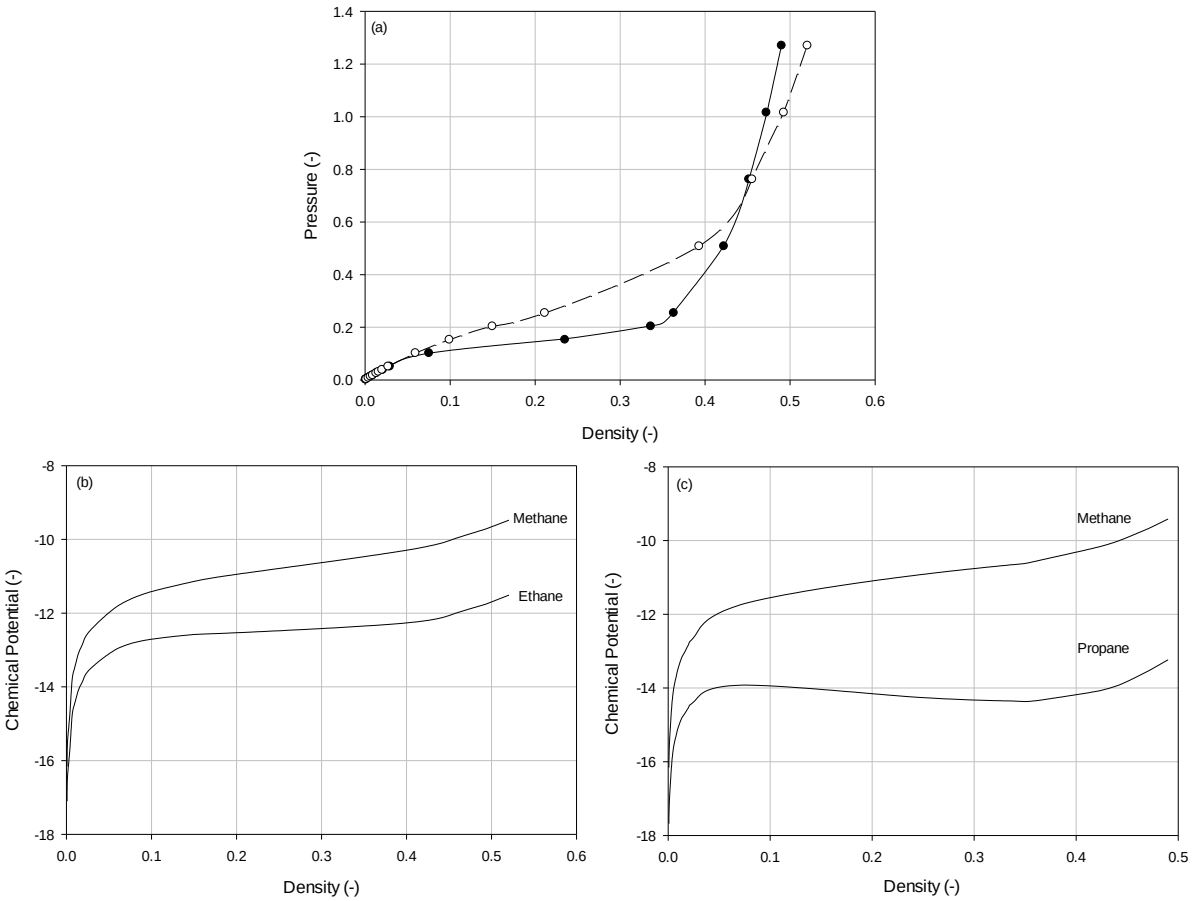

Figure 3-11 (a) Pressure plot of methane/ethane mixture (dashed line) and methane/propane mixture (solid line). The symbols show the input pressure. (b) Chemical potentials of methane/ethane mixture; and (c) Chemical potentials of methane/propane mixture.

Figure 3-12 compares the chemical potentials calculated from *NPT-kMC* with the ideal gas chemical potential for the ternary system methane/ethane/propane system at 300K. Except at very low densities, the ideal gas chemical potentials (dashed line) and the pure component (dotted line) chemical potentials deviate from the kMC chemical potentials (solid line) and is greater for the heavier components.

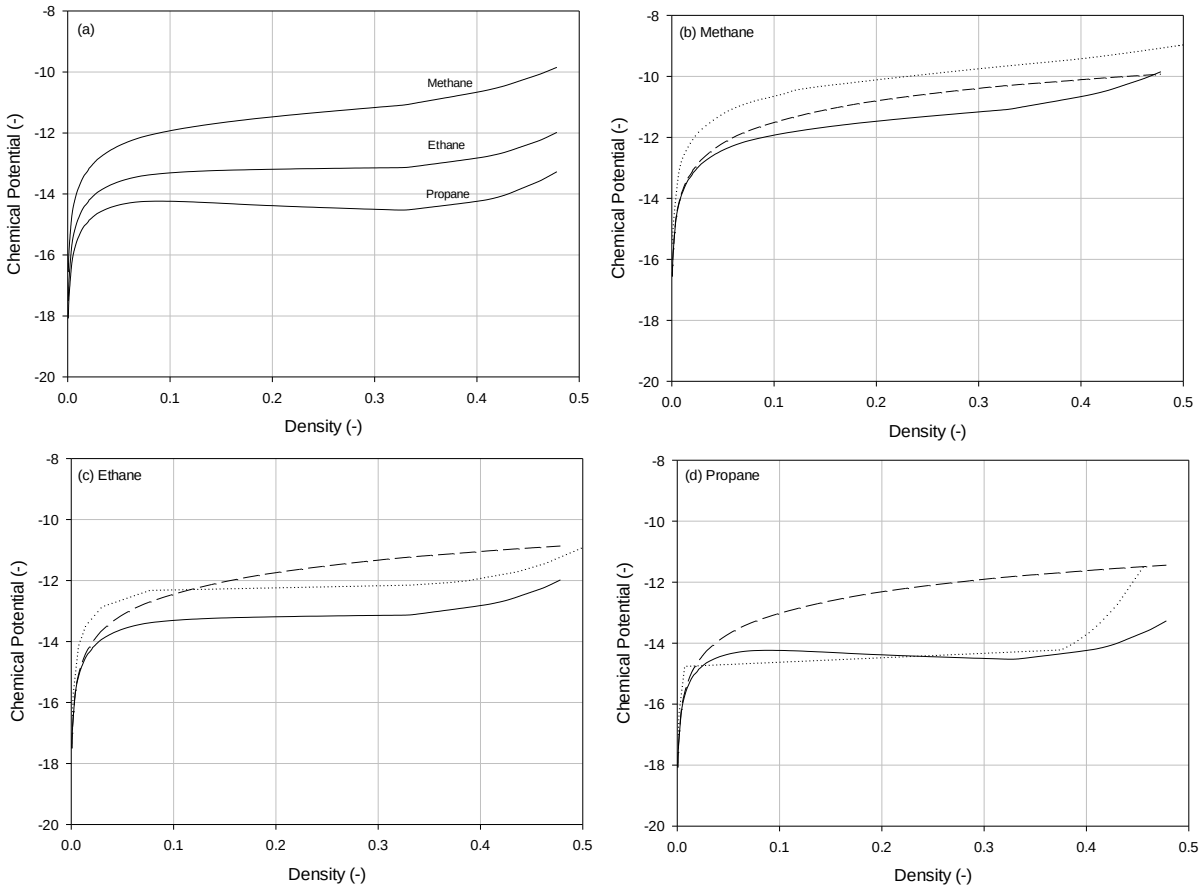

Figure 3-12 Chemical potential versus total density for a of methane/ethane/propane mixture. Solid line: *NPT-kMC* results; dashed line ideal gas chemical potential. The dotted line is the chemical potential of the pure component.

References

1. Tegeler, C., R. Span, and W. Wagner, *A New Equation of State for Argon Covering the Fluid Region for Temperatures From the Melting Line to 700 K at Pressures up to 1000 MPa.* J. Phys. Chem., 1999. **28**(3): p. 779-850.
2. Johnson, J.K., J.A. Zollweg, and K.E. Gubbins, *The Lennard-Jones Equation of State Revisited.* Molecular Physics, 1993. **78**(3): p. 591-618.

Chapter 4. Grand Canonical kinetic Monte Carlo

4.1. Introduction

The grand canonical (GC) ensemble is the only Monte Carlo (MC) ensemble which allows the number of particles to fluctuate, making it the ensemble of choice for simulating an open system. For example, adsorption is one of the many studies that utilise GCMC [1-4] as the principal simulation tool. In this ensemble, the number of particles of each component fluctuates such that its chemical potential is equal (within statistical error) to the specified chemical potential. Since a set of chemical potentials of all components is the input to the grand canonical simulation, these must be calculated at a given temperature and pressure. For simple spherical molecules, such as argon, the chemical potential can be calculated from the EOS of Johnson *et al* [5]. However, for more complex molecules, this set of chemical potentials has to be determined form the *NPT* ensemble as addressed in Chapter 3.

A kinetic Monte Carlo scheme for a grand canonical ensemble was developed by Ustinov and Do [6] and was applied to adsorption on a surface and a slit pore. However, the method was only developed for pure component systems. In this chapter, a new scheme to deal with mixtures has been developed the first time. The new scheme uses the *sub-NVT* block concept developed in Chapter 3 but the volume change move used in the *NPT* ensemble, is replaced with a move in which molecules are exchanged with the surroundings.

4.2. Simulation Details

As in the *NPT-kMC* in Chapter 3, the insertion-deletion steps in the grand ensemble are made by invoking the concept of *sub-NVT* ensembles. Based on the findings in Chapter 3 where various ways of carrying out the volume change move were explored, only one algorithm to execute the insertion and deletion move was considered. In this, a comparison of the *block average* chemical potentials (activity), instead of the instant chemical potentials, with the specified chemical potentials is made.

The *block average* activity of a component β in a *sub-NVT* block of M local displacement moves is calculated as follows:

$$\left\langle \alpha_{\beta} \right\rangle = \frac{\sum_{j=1}^{M} \Delta t_j \; \alpha_{\beta,j}}{\sum_{j=1}^{M} \Delta t_j} = \frac{\sum_{j=1}^{M} \Delta t_j \; \alpha_{\beta,j}}{T_M} \qquad \text{Eq. 4-1}$$

where $\alpha_{\beta,j}$ is the activity of the component β at the configuration j, with duration given by Equation 2-11 and T_M is the total duration of the M configurations in the *sub-NVT* block. These *block average* chemical potentials (activities) are then used for the exchange move. For a set of specified chemical potentials of all components $\left\{\left(\mu_{\beta} - \mu_{\beta}^{intra}\right)^{*}\right\}$, where the superscript * denotes "specified", the specified activity of the component β is:

$$\alpha_{\beta}^{*} = \frac{1}{\Lambda_{\beta}^{3}} \exp\left[\frac{\left(\mu_{\beta} - \mu_{\beta}^{intra}\right)^{*}}{kT}\right] \qquad \text{Eq. 4-2}$$

At the end of a *sub-NVT* block, we calculate the average activities for all components according to Equation 4-1 and the exchange decision rests on the comparison between these and the specified values from Equation 4-2. First, a component is selected at random so that all components have an equal chance for the exchange move. Let this component be the component β. The exchange could be done in a deterministic manner as follows: If the *block average* activity of the component β is less than the specified value, $\left\langle \alpha_{\beta} \right\rangle < \alpha_{\beta}^{*}$, a molecule of that component is added; otherwise a molecule is selected from the sub-population of component β using the Rosenbluth algorithm and is deleted. However, to maintain the stochastic character of *kMC*, we implement the Rosenbluth algorithm [7] in the exchange decision as follows: For a configuration j in a *sub-NVT* block, we calculate the molecular activity, $\gamma_{i,j}^{\beta}$, of molecule i of component β:

$$\gamma_{i,j}^{\beta} = \frac{\nu_{i,j}^{\beta}}{V} \qquad \text{Eq. 4-3}$$

At the end of the *sub-NVT* block, the *block average* molecular activity of this molecule is:

$$\left\langle \gamma_{i}^{\beta} \right\rangle = \frac{\sum_{j=1}^{M} \Delta t_j \; \gamma_{i,j}^{\beta}}{\sum_{j=1}^{M} \Delta t_j} = \frac{\sum_{j=1}^{M} \Delta t_j \; \gamma_{i,j}^{\beta}}{T_M} \qquad \text{Eq. 4-4}$$

The *block average* activity of component β from molecule 1 up to molecule k is:

$$\left\langle \alpha_{\beta,k} \right\rangle = \sum_{\substack{i=1 \\ i\in\beta}}^{k} \left\langle \gamma_i^{\beta} \right\rangle \qquad \text{Eq. 4-5}$$

Since the activity is specified in a grand canonical ensemble we define an auxiliary activity as:

$$\alpha_{\beta}^{aux} = \left\langle \alpha_{\beta} \right\rangle + \alpha_{\beta}^{*} \qquad \text{Eq. 4-6}$$

The decision to insert or delete is based on the inequality:

$$\left\langle \alpha_{\beta,k-1} \right\rangle \quad \leq \quad rand \times \alpha_{\beta}^{aux} \quad < \quad \left\langle \alpha_{\beta,k} \right\rangle \qquad \text{Eq. 4-7}$$

which determines the value of k. If k is less than or equal to N_β, the system is too energetic with respect to this component, and the k^{th} molecule is then deleted from the system. On the other hand, if $k=N_\beta+1$, a molecule is inserted into the system at a random position and given a random orientation.

4.3. Size of a *sub-NVT* block

Similar to *NPT-kMC* in Chapter 3, the size of the *sub-NVT* block has to be determined in such a way that the *block average* activity gives a reasonably accurate description of the system. A *canonical-kMC* simulation of a liquid argon at 120K for a series of densities was done to estimate the block size for a system of 500 particles. Figure 4-1 shows that it would require approximately 200,000 displacement moves for the activity to relax the system at a reduced density of 0.74, representing a liquid phase above the saturation density (0.7). This means that each particle has statistically 400 moves. It is also obvious that more displacement moves are required for higher densities.

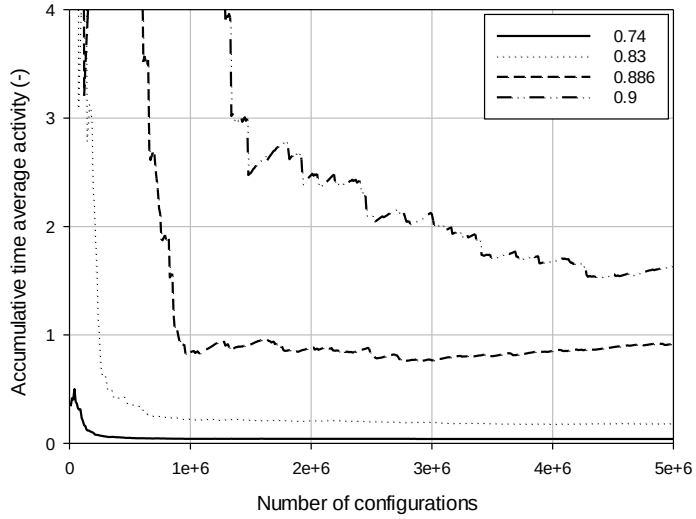

Figure 4-1 Evolution of activity with configuration

To further reduce the CPU time for a simulation, a series of different block sizes for liquid argon (reduced density of 0.71) at 120K was simulated in the grand canonical ensemble and the results plotted in Figure 4-2. As expected, the fluctuation decreases as the block size increases. 100 displacement per particle per block is seen to be the optimal choice as the larger block size does not yield any significant improvement.

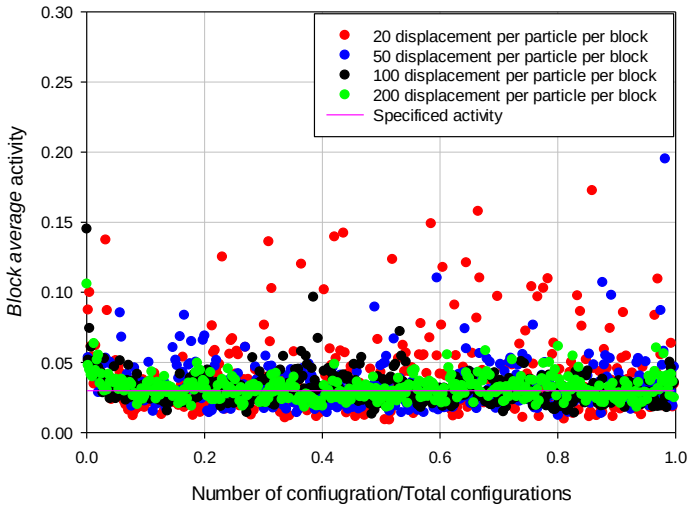

Figure 4-2 The *block average* activity of different block size

4.4. Application to pure gas and mixtures

Simulations for argon were run in a cubic box at supercritical temperatures of 240K and 400K, and 400K for methane, ethane, propane and methane/ethane/propane mixture. The dimensions of the

simulation box in Table 4-1 were selected in such a way that there will be between 100-300 particles at the end of the simulation. The size of a *sub-NVT* block in the equilibration and sampling stages was taken to be 100 displacement move per particle.

Argon					
Fluid Density* (-)	$\rho < 0.001$	$0.001 < \rho \leq 0.01$	$0.01 < \rho \leq 0.04$	$0.04 < \rho \leq 0.2$	$0.2 < \rho$
Box Length (nm)	20	15	10	5	3
Methane/Ethane/Propane mixture at 400K					
Total Density* (-)	$\rho < 0.001$	$0.001 < \rho \leq 0.01$	$0.01 < \rho \leq 0.04$	$0.04 < \rho \leq 0.2$	$0.2 < \rho$
Box Length (nm)	20	15	10	5	3

Table 4-1 Dimensions of the simulation box. *Density was determined from *NPT-kMC* simulations

Figure 4-3 shows the pressure-density plots for argon obtained from the new grand canonical simulations and compares with the *NPT-kMC* result determined in Chapter 3. Both the calculated reduced pressure and reduced density are in excellent agreement with the corresponding results from *NPT-kMC*.

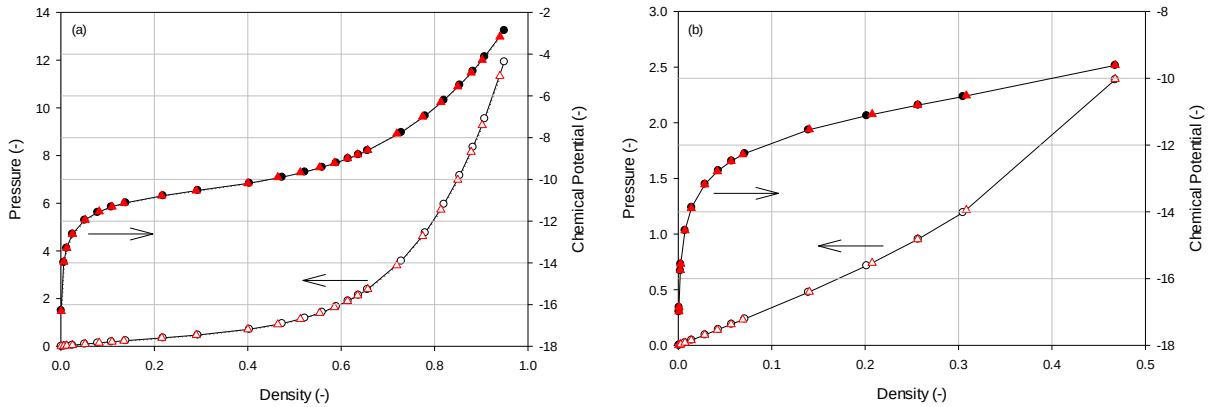

Figure 4-3 Simulated properties for argon at (a) 240K and (b) 400K, reduced pressure (unfilled shapes) and chemical potential (filled shapes) as functions of total reduced density. Triangles are results obtained from *GC-kMC* and solid lines with circles are results obtained from *NPT*-kMC.

The *GC-kMC* and *NPT-kMC* results for the pure components and equimolar methane/ethane/propane mixtures are shown in Figure 4-4, and once again are in excellent agreement for both pressure and chemical potential throughout the range of density tested.

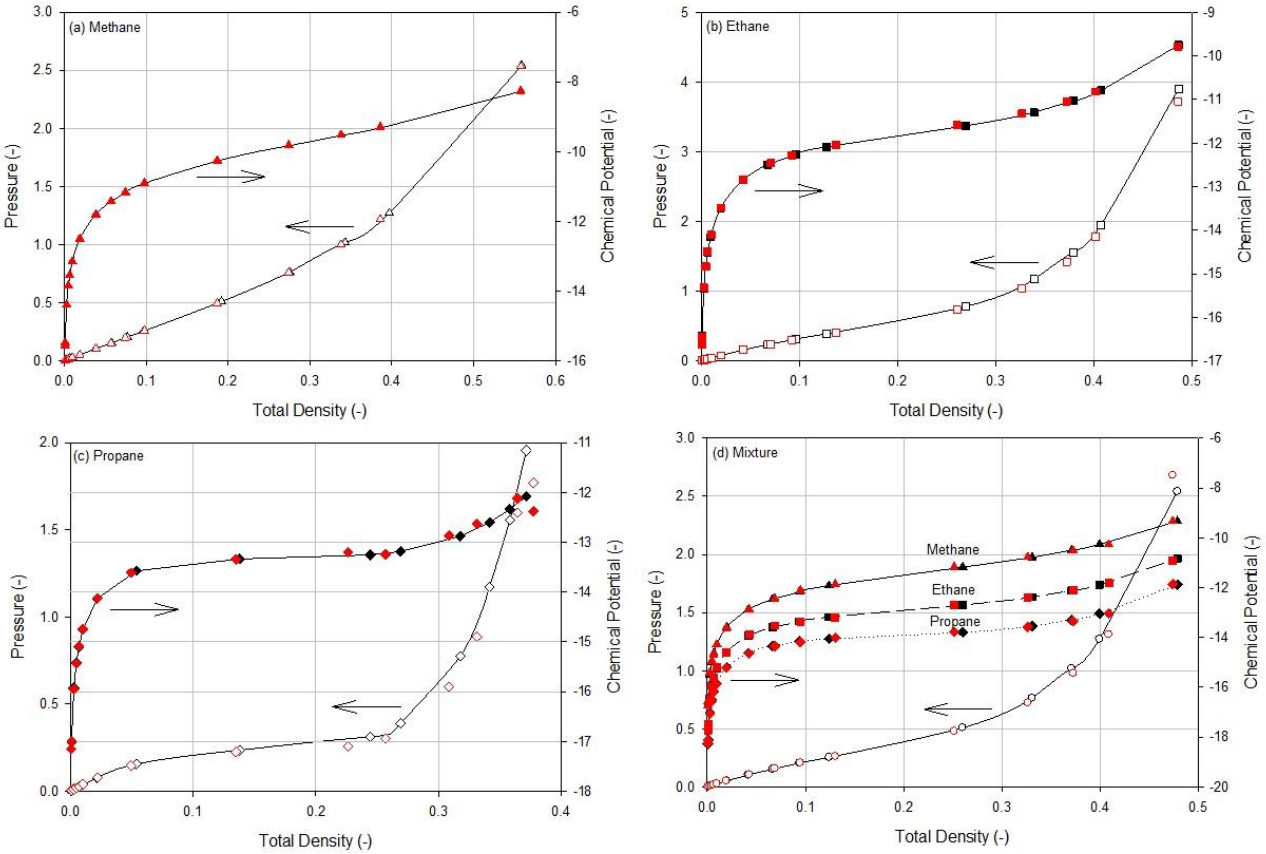

Figure 4-4 Simulated reduced pressure (unfilled shapes) and chemical potential (filled shapes) at 400K as functions of total density for (a) Methane (triangle); (b) Ethane (square); (c) Propane (diamond); and (d) methane/ethane/propane mixture. Red symbols are results from *GC-kMC* and lines with black symbols are obtained from *NPT-kMC*.

References

1. Ohba, T. and K. Kaneko, *GCMC study on relationship between DR plot and micropore width distribution of carbon.* Langmuir, 2001. **17**(12): p. 3666-3670.
2. Zeng, Y., D.D. Do, and D. Nicholson, *Existence of Ultrafine Crevices and Functional Groups along the Edge Surfaces of Graphitized Thermal Carbon Black.* Langmuir, 2015. **31**(14): p. 4196-4204.
3. Klomkliang, N., D.D. Do, and D. Nicholson, *Scanning curves in wedge pore with the wide end closed: Effects of temperature.* AIChE Journal, 2015.
4. Phadungbut, P., D.D. Do, and D. Nicholson, *Undulation Theory and Analysis of Capillary Condensation in Cylindrical and Spherical Pores.* The Journal of Physical Chemistry C, 2015.
5. Johnson, J.K., J.A. Zollweg, and K.E. Gubbins, *The Lennard-Jones Equation of State Revisited.* Molecular Physics, 1993. **78**(3): p. 591-618.
6. Ustinov, E.A. and D.D. Do, *Simulation of gas adsorption on a surface and in slit pores with grand canonical and canonical kinetic Monte Carlo methods.* Phys Chem Chem Phys, 2012. **14**(31): p. 11112-8.
7. Frenkel, D. and B. Smit, *Understanding molecular simulation : From algorithms to applications.* Second ed. Computational Science Series, ed. D. Frenkel, et al. 2002, San Diego: Academic Press. 638.

Chapter 5. Gibbs Canonical kinetic Monte Carlo

5.1. Introduction

Simulations of a bulk fluid at temperatures below its critical temperature with a canonical (*NVT*) ensemble yield a loop of chemical potential (or pressure) versus density, of van der Waals type, with three distinct branches: (1) stable and metastable branch where the chemical potential increases with density, (2) unstable branch where the chemical potential decreases with density and (3) equilibrium branch where the chemical potential is constant with respect to density (Figure 5-1a). The constant chemical potential of the equilibrium branch is the coexistence chemical potential of the two phases in contact to each other [1]. On the unstable branch chemical potential is dependent on the choice of the system parameters, for example the box size as shown in Figure 5-1b.

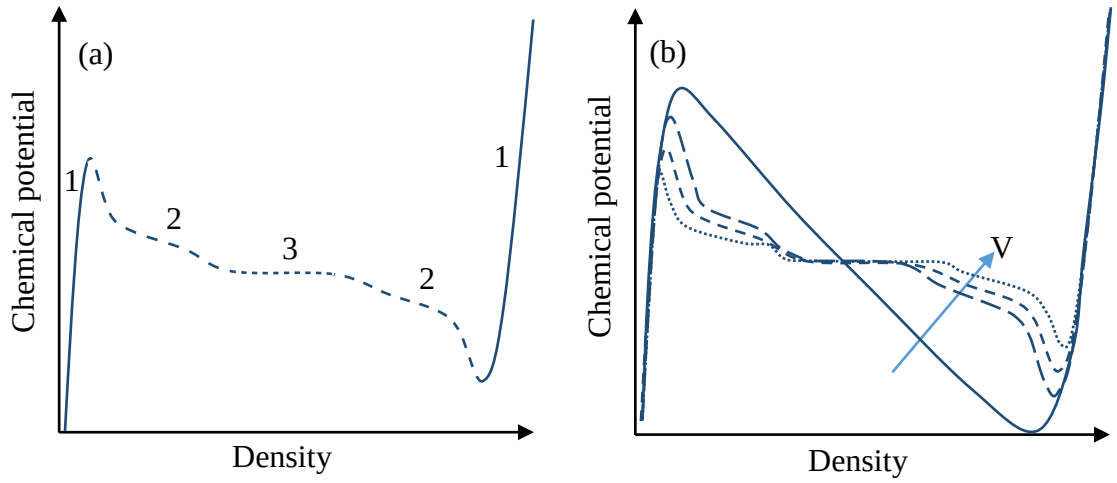

Figure 5-1 Van der Waals loop (a) with three distinct branches: 1 - stable and metastable region, 2 - unstable region and 3 – the phase co-existing region, and (b) dependency on box size

Extending the horizontal section of the equilibrium branch to both sides intersects with the stable-metastable branches of the vdW loop at the saturation gas and liquid densities. This, in principle, will provide the saturation densities and pressure, but this is an extremely expensive course. Simulations using *NPT* ensembles, as described in Chapter 3, only trace the stable and metastable branches of pressure versus density, and likewise simulations using

μVT ensembles, as described in Chapter 4, will only trace the stable and metastable branches of chemical potential versus density. Like the *NVT* ensemble, the simulation of these ensembles is very expensive and is not recommended for the determination of saturation properties. To this end, Panagiotopoulos in 1987 [2] and in subsequent papers [3-5] developed a very ingenious ensemble to obtain these properties in a single simulation, avoiding the huge costs associated with the other ensembles. This ensemble is known as the "Gibbs" ensemble in honour of Josiah Willard Gibbs, who developed the thermodynamic foundations of phase equilibria. The algorithm used by Panagiotopoulos rests on the importance sampling of Metropolis. In the spirit of using kinetic Monte Carlo we develop in this chapter, for the first time, the so-called *Gibbs-kMC*. Like the traditional *Gibbs-MC*, the *kMC* simulation involves two boxes representing the two phases of a bulk fluid, and to achieve the chemical and mechanical equilibrium interchange of molecules between the two boxes and changing their volumes are necessary: the interchange is similar to the grand canonical of Chapter 4 while the volume change is similar to the *NPT* of Chapter 3.

5.2. Simulation Details

The algorithm for the *Gibbs-kMC* simulation is similar to that developed in Chapters 3 and 4. The *sub-NVT* ensembles (with local displacement in each box as the only move) were used as a block in a chain of configurations, and the so called *block average* properties were then utilized to execute the transfer of molecules and the volume change to achieve equal chemical potential and pressure in a sufficiently long chain of configurations. Thus it could be viewed that the chain is composed of a sequence of *NVT* blocks with either mass exchange or volume change at the end of each block. The probability of choosing either mass exchange or volume change will be discussed in Section 5.4.

The local displacement, the mass interchange and the volume change moves are given below:

1. Local move: This is carried out in each *sub-NVT* block, and its purpose is to relax the two boxes to "equilibrium" as described in Chapter 2.3. A molecule is selected in each box and displaced randomly throughout the volume of its respective box. At the end of the block, the *block average* thermodynamic properties (pressure, chemical potentials and configurational energy) of each box are calculated using Equation 2-27.
2. Exchange move: The purpose of this move is to equalize the chemical potentials of each component β in the two boxes (chemical equilibrium). At the end of a

sufficiently long *sub-NVT* block, the time average chemical potentials (or activities) of all components are "expected" to be the same, written below for component β (the selection of component β is done at random, for example in a binary system, a component is selected with 0.5 probability):

$$\left\langle \alpha_\beta^{(\mathrm{I})} \right\rangle = \left\langle \alpha_\beta^{(\mathrm{II})} \right\rangle \qquad \text{Eq. 5-1}$$

The exchange move could be done in a deterministic manner by comparing the *block average* activity. If the *block average* activity of Box 1 is less than that of Box 2, a molecule of component β is selected in Box 2 and moved to Box 1. However, to maintain the stochastic nature of *kMC*, the Rosenbluth algorithm is implemented and this is done as follows: The auxiliary activity is defined as the sum of the *block average* activities of the two boxes:

$$\alpha_\beta^{aux} = \left\langle \alpha_\beta^{(\mathrm{I})} \right\rangle + \left\langle \alpha_\beta^{(\mathrm{II})} \right\rangle \qquad \text{Eq. 5-2}$$

If the *block average* activity of Box 1 is less than or equal to $rand \times \alpha_\beta^{aux}$:

$$\left\langle \alpha_\beta^{(\mathrm{I})} \right\rangle \le rand \times \alpha_\beta^{aux} \qquad \text{Eq. 5-3}$$

a molecule is selected from the sub-population of component β in Box 2, using the Rosenbluth scheme, and moved to Box 1; otherwise a molecule is selected in Box 1 and move it to Box 2. The durations for the configurations of the two boxes, after the exchange move, are calculated as in Equation 2-12.

3. Volume move: The purpose of this move is to equalize the pressures of the two boxes (mechanical equilibrium). This could be done in three ways: (a) using the instant pressures of two boxes at the end of a block (b) using the *block average* pressures, and (c) using the averages of the time averaged pressures of all blocks between two consecutive volume moves, as shown in the equation below.

$$\left[\left\langle P^{(\mathrm{I})} \right\rangle\right] = \frac{1}{N_{ex}} \sum_{n=1}^{N_{ex}} \left\langle p^{(\mathrm{I})} \right\rangle_n \qquad \left[\left\langle P^{(II)} \right\rangle\right] = \frac{1}{N_{ex}} \sum_{n=1}^{N_{ex}} \left\langle p^{(II)} \right\rangle_n \qquad \text{Eq. 5-4}$$

where *n* is the *n-th* block in a sequence of N_{ex} blocks between two consecutive volume moves. To carry out the volume change, an auxiliary pressure is defined as:

$$P^{aux} = P^{(\mathrm{I})} + P^{(\mathrm{II})} \qquad \text{Eq. 5-5}$$

where the pressures in the RHS of the above equation could be one of the three different uses of pressure as discussed in the above paragraph. A box is chosen to expand (and the other is contracted to maintain constant total volume) as follows. If $P^{(\mathrm{I})} > rand \times P^{aux}$, then Box 1 is expanded, because its pressure is statistically high, according to the following equation

$$\begin{aligned} V'^{(\mathrm{I})} &= V^{(\mathrm{I})} + rand \times \Delta V_{\max} \\ V'^{(\mathrm{II})} &= V_{total} - V'^{(\mathrm{I})} \end{aligned} \qquad \text{Eq. 5-6}$$

where *rand* is a random number and ΔV_{max} is the maximum allowable volume change. On the other hand, if $P^{(\mathrm{I})} \le rand \times P^{aux}$, Box *2* is expanded instead using Equation 5-6. Similar to the *NPT-kMC*, the cut-off radius is adjusted to half of the new box length after a volume change move is done. The maximum change in volume (ΔV_{max}) has been addressed in Chapter 3.3.

5.3. The size of a *sub-NVT* block

Like the NPT and μVT ensembles, the choice of the size of a *sub-NVT* block before an exchange move or volume is made, is very important. To determine this size, a *canonical-kMC* simulation of a bulk liquid at saturation was carried out and the control charts of the running time average activity and pressure were observed. The bulk liquid densities were taken from Tegeler *et al.* [6] and 250 particles were used in the simulation box. Figure 5-2 shows that the number of configurations required to relax the system increases with lower temperatures, due to higher saturation densities. It is very interesting to make an observation that the pressures for very low temperatures, 70K and 60K, take about 4 times longer to stabilize because of the system is solid-like at these temperatures. With the exception of the solid-like phase, we have found that the optimum size of a *sub-NVT* is 100 local displacement moves per particle, and this will be used in the subsequent simulations.

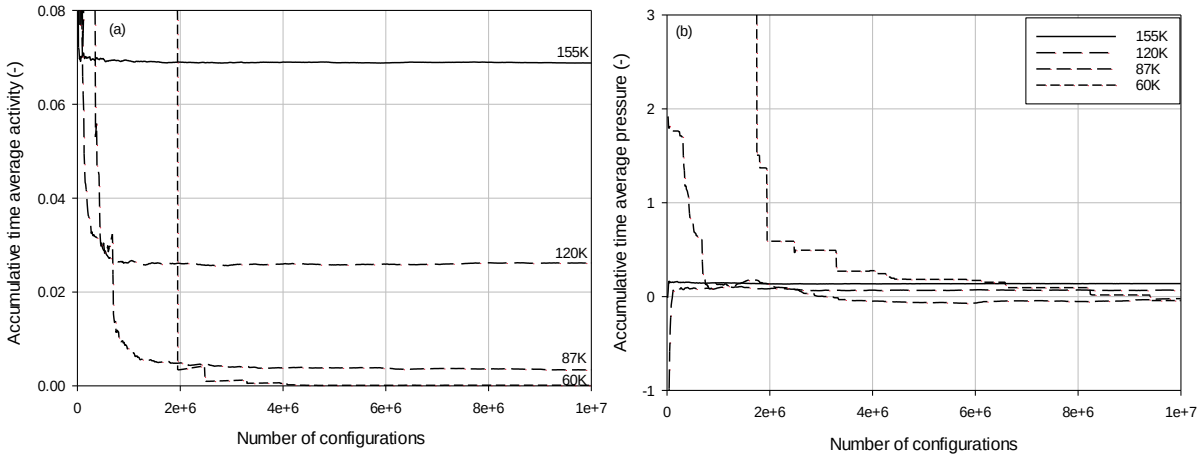

Figure 5-2 Accumulative time average (a) activity and (b) pressure of a series of temperatures against number of configurations.

5.4. Percentage of exchange and volume change moves

At the end of a *sub-NVT* block, either an exchange move or a volume move were carried out, but what are their optimal probabilities? A high percentage of volume move could lead to the liquid box becoming too small in size and this is undesirable because: (1) the cut-off radius is too small to get accurate calculation of energy, (2) the number of molecules in the liquid box is too low and (3) the total configuration energies have to be recalculated each time a volume change is made because of the scaling of the positions of all molecules. Therefore, a good choice would be one that has a low probability for the volume move. This is illustrated in Figure 5-3, the *Gibbs-kMC* simulation results at 120K with 250 argon molecules in each cubic box having a linear dimension of 3.2nm. It is shown that simulations with a high percentage of volume moves fail to describe the gas phase correctly, and as expected the ones with 0.01 probability of volume moves give the best splitting into two phases of correct respective densities. This choice will be used in the remaining parts of this chapter.

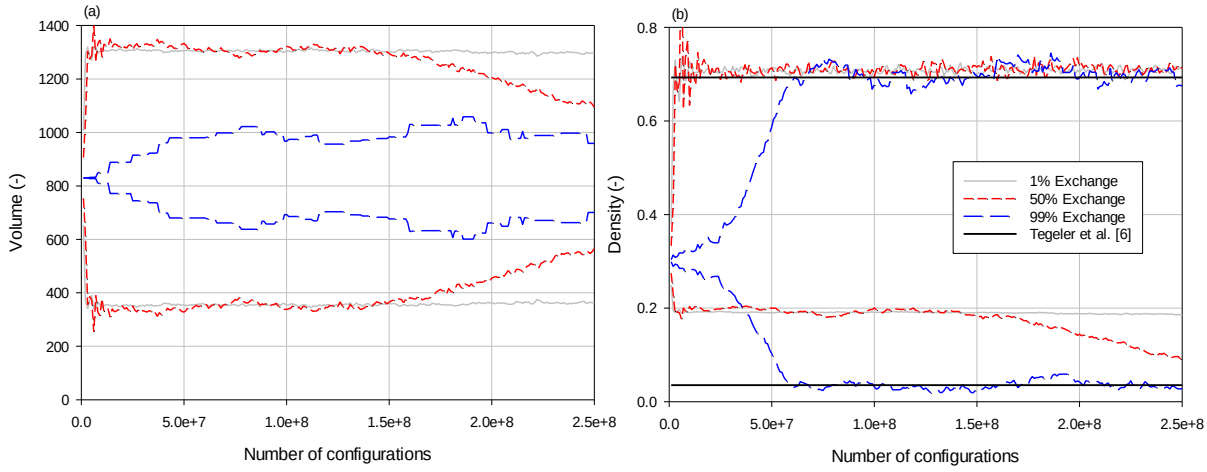

Figure 5-3 Series of different percentage of exchange move at 120K, the simulations uses *block average* pressure for volume move decision and activity with Rosenbluth selection for exchange move decision.

5.5. Scheme for volume change move

The simulation results for the system of argon at 120K with 250 molecules in each cubic box of 3.2nm linear dimension are shown in Figure 5-4 to show the different choices of pressure, as detailed in Section 5.2. Since all of the schemes give a similar result, the *block average* pressure will be selected for the decision of volume change move.

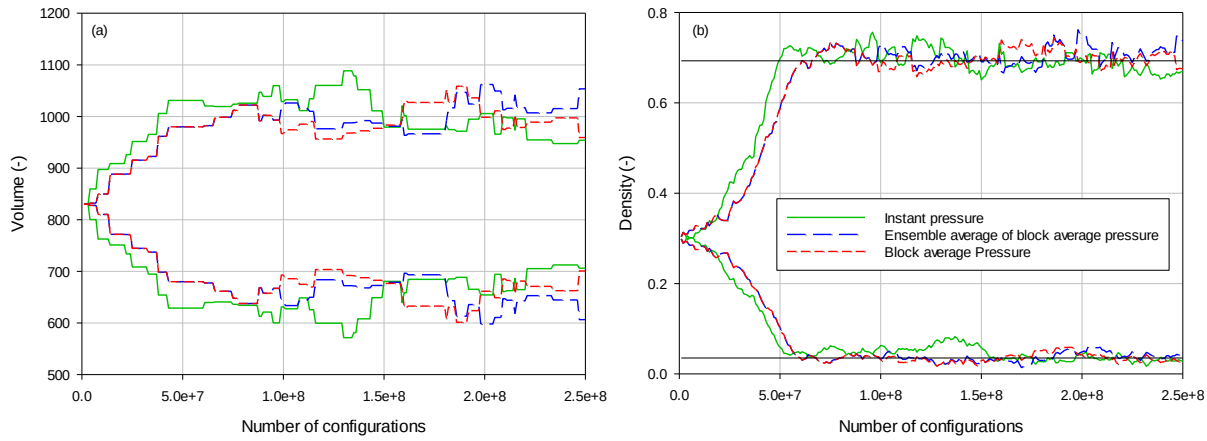

Figure 5-4 Different schemes for volume change move at 120K. The black vertical line represent the density of coexisting liquid and gas argon by Tegeler *et al.* [6] at 120K.

5.6. *Block average* activity or logarithm of block average activity

As shown in Chapter 4 that the block average activity of the liquid phase fluctuates with a very large amplitude. The possibility of using the logarithm of the block average activity in the mass exchange move are explored in this section, i.e. the decision of the direction of molecule transfer is done as in Equations 5-2 and 5-3, by replacing $\left\langle \alpha_{\beta}^{\Omega} \right\rangle$ by $\ln\left\langle \alpha_{\beta}^{\Omega} \right\rangle$.

The simulation results of the *block average* activity and logarithm of the *block average* activity are shown in Figure 5-5 for a system of argon at 120K and 250 molecules in each cubic box of 3.2nm linear dimension. Both choices give a similar result and it is found that the deterministic route to move molecules requires a lower number of configurations than the random Rosenbluth route.

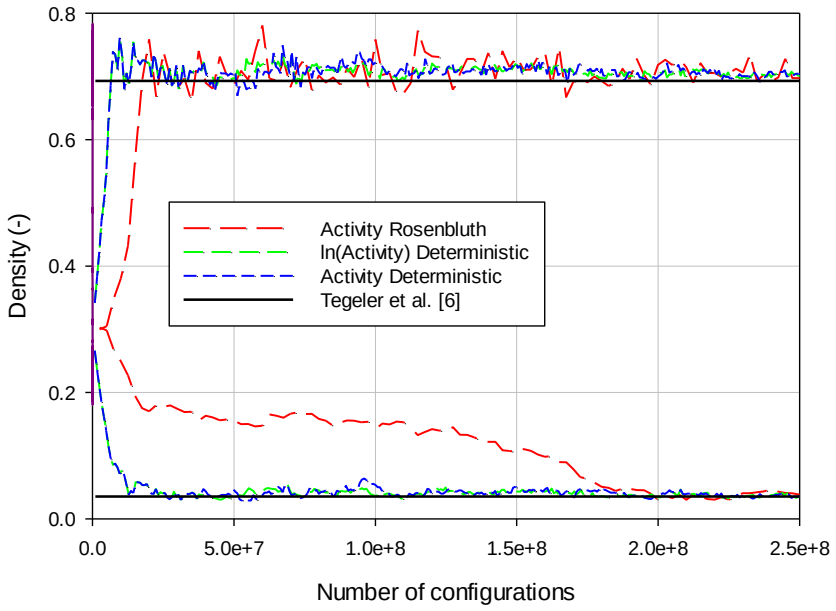

Figure 5-5 Different schemes for exchange move at 120K

5.7. Application to Argon

Figure 5-6 shows the simulation results of the liquid vapour equilibrium of argon as plots of densities of the two phases as a function of temperature. The results obtained in this investigation are comparable to those obtained with the conventional *Gibbs-MC* of Panagiotopoulos [3], although there are some deviations between the two results at temperatures close to the critical points. These are most likely due to the high thermal

fluctuations. This is the subject of further investigation as one of the issues recommended in the Recommendation section.

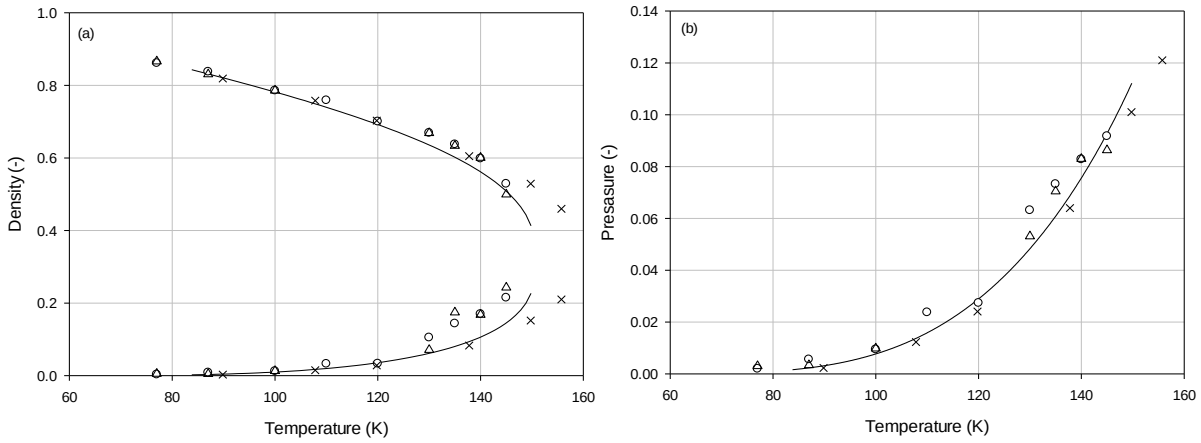

Figure 5-6 Liquid-vapour equlibrium of argon, triangles and circles are the results obtained by *GEkMC* using the *block average* pressure (triangle) and ensemble average of the *block average* pressure (circle) for the decision of volume change move, crosses are results obtained by *GEMC* simulation done by Panagiotopoulos *et al.* [3] and solid line refers to Tegeler *et al.* [2].

References

1. Schrader, M., P. Virnau, and K. Binder, *Simulation of vapor-liquid coexistence in finite volumes: A method to compute the surface free energy of droplets.* Physical Review E, 2009. **79**(6): p. 061104.
2. Panagiotopoulos, A.Z., *Direct determination of phase coexistence properties of fluids by Monte Carlo simulation in a new ensemble.* Molecular Physics, 1987. **61**(4): p. 813-826.
3. Panagiotopoulos, A.Z., N. Quirke, M. Stapleton, and D.J. Tildesley, *Phase equilibria by simulation in the Gibbs ensemble: Alternative derivation, generalisation and application to mixture and membrane equilibria.* Molecular Physics, 1988. **63**(4): p. 527-545.
4. Panagiotopoulos, A.Z., *Monte Carlo methods for phase equilibria of fluids.* J. Phys.: Condens. Matter, 2000. **12**(Copyright (C) 2011 American Chemical Society (ACS). All Rights Reserved.): p. R25-R52.
5. Panagiotopoulos, A.Z., *Exact calculations of fluid-phase equilibria by Monte Carlo simulation in a new statistical ensemble.* International Journal of Thermophysics, 1989. **10**(2): p. 447-457.
6. Tegeler, C., R. Span, and W. Wagner, *A New Equation of State for Argon Covering the Fluid Region for Temperatures From the Melting Line to 700 K at Pressures up to 1000 MPa.* J. Phys. Chem., 1999. **28**(3): p. 779-850.

Chapter 6. Conclusions and Recommendations

6.1. Conclusions

The aim of this thesis is to develop new simulation tools to determine the chemical potential of mixtures accurately. This objective has been achieved with the new method proposed in Chapter 3 which performs *kMC* simulations in the *NPT* ensemble. Two types of move are required to perform the *NPT-kMC*: displacement and volume change. Displacement moves are made using the Rosenbluth algorithm with no rejection. Volume changes need careful calibration to establish an optimum value for the maximum allowable volume change, ΔV_{max}. The concept of a *sub-NVT* ensemble within the *NPT* simulation is introduced which improves the accuracy of calculated properties. The technique has been applied to pure argon and to mixtures of methane with ethane and with ethane and propane.

As a validation process for the chemical potential obtained in the *NPT-kMC* simulations, a new *grand canonical* kinetic Monte Carlo procedure was developed. A key feature is the improvement in the calculation of chemical potential of dense phase fluid, gained by employing *sub-NVT* ensembles within the grand canonical simulation. The new procedure is illustrated by simulations of supercritical argon, methane, ethane and propane and their mixtures. The new *GC-kMC* scheme is tested by comparison with *NPT-kMC* simulations and excellent agreement has been achieved.

Finally, a novel method to predict the properties of coexisting fluids is proposed via *Gibbs canonical* kinetic Monte Carlo. The concept of *sub-NVT* ensembles were once again introduced and require three types of move: displacement, exchange and volume change. The displacement move is done to achieve internal equilibrium within each of the boxes, the exchange move and the volume change move are done to achieve chemical and mechanical equilibrium between two boxes, respectively. Once this is done, the two boxes represent the two coexisting phases of different densities. This procedure was applied to argon and the coexistence was achieved with reasonably accurate densities, pressure and chemical potential of the two phases.

6.2. Recommendations

The progress of research into mixtures in fluid and adsorption systems is somewhat limited because of the difficulty in getting the chemical potential of mixtures, which are required in a simulation of an open system where temperature and pressure are specified. The *NPT* ensemble developed in this thesis provide a fundamental step in this direction. Therefore, it is expected that it will provide a tool to study bulk fluids and adsorption of many systems of practical interest in engineering:

- Better understanding with microscopic behaviour of bulk mixtures in terms of the roles of attraction and repulsion in pressure and chemical potential, relative to ideal gas pressure and chemical potential.
- Adsorption of complex fluids and its mixtures, for example mixtures of polar and non-polar compounds.
- Adsorption of mixtures in simple pores to build a foundation of mixture adsorption, followed by adsorption in complex pores, for example ink-bottle pores and disordered amorphous solids.
- Vapour liquid equilibrium of mixtures over a wide range of temperatures.
- Extend *Gibbs-NVT-kMC* to simulate bulk mixtures. The *sub-NVT* concept introduced in this work will be further explored to optimise the procedure in order to speed up the calculation. In addition, it could be implemented into a new ensemble of *Gibbs-NPT-kMC.*